INVESTIGATION AND MODIFICATION OF HYDROKINETIC SAVONIUS TURBINE FOR LOW WATER SPEEDS

A THESIS SUBMITTED TO
THE BOARD OF GRADUATE PROGRAMS
OF
MIDDLE EAST TECHNICAL UNIVERSITY, NORTHERN CYPRUS CAMPUS

BY

CHIEDOZIE AUGUSTINE IKE-OFFIAH

IN PARTIAL FULFILLMENT OF THE REQUIREMENTS
FOR
THE DEGREE OF MASTER OF SCIENCE
IN SUSTAINABLE ENVIRONMENT AND ENERGY SYSTEMS PROGRAM

NOVEMBER, 2022

Approval of the Board of Graduate Programs

Prof. Dr. Cumali Sabah

Chairperson

I certify that this thesis satisfies all the requirements as a thesis for the degree of Master of Science

Assoc. Prof. Dr. Ceren Ince

Program Coordinator

This is to certify that we have read this thesis and that in our opinion it is fully adequate, in scope and quality, as a thesis for the degree of Master of Science.

Assoc. Prof. Dr. Elif Oğuz	Assist. Prof. Dr. Ali Atashbar Orang
Co-Supervisor	Supervisor

Examining Committee Members

Assist. Prof. Dr. Lida Ebrahimi Vafaei	AERT/NEU	
Assist. Prof. Dr. Ali Atashbar Orang	Mech/METU NCC	
Assist. Prof. Dr. Canras Batunlu	EEE/METU NCC	

I hereby declare that all information in this document has been obtained and presented in accordance with academic rules and ethical conduct. I also declare that, as required by these rules and conduct, I have fully cited and referenced all material and results that are not original to this work.

Name, Last name: Chiedozie Augustine Ike-Offiah
Signature:

ABSTRACT

INVESTIGATION AND MODIFICATION OF HYDROKINETIC SAVONIUS TURBINE FOR LOW WATER SPEEDS

Ike-Offiah, Chiedozie Augustine
Master of Science, Sustainable Environment and Energy Systems Program
Supervisor: Assist. Prof. Dr. Ali Atashbar Orang
Co-Supervisor: Assoc. Prof. Dr. Elif Oğuz

November 2022, 61 pages

With the ever-growing global interest in reducing greenhouse gases such as CO_2, renewable energy options present a good energy alternative. Not only are they a sustainable option in their operational period, but they also have a low implementation cost especially, when compared to conventional fossil fuel sources. Hydrokinetic turbines have the advantages of energy predictability, relatively low visual impact, a high energy density, high capacity factor, and ease of manufacture, in addition to the low cost of deployment. This study focuses on the investigation and modification of Savonius hydrokinetic turbines operating at a low speed. ANSYS CFX as the commercial solver is utilized to simulate the transient flow field using the sliding-mesh technique, along with the proper boundary conditions. Important controlling parameters include the aspect ratio (AR), overlap ratio, and shape of the blades. The numerical set up is validated by comparing the results with the results of available studies in literature. The elliptical-shaped blade design, is proposed in this study since it generates higher positive torque in comparison with that of the conventional one. The optimal overlap ratio is found for the modified design based on available literature, while the optimal AR is detected by testing different AR values.

Keywords: Renewable Energy, Hydrokinetic Energy Systems, Computational Fluid Dynamics (CFD), Savonius turbine, Numerical Analysis.

ÖZ

DÜŞÜK AKIM HIZINDA HİDROKİNETİK SAVONIUS TÜRBİNİN İNCELENMESİ VE MODİFİKASYONU

Ike-Offiah Chiedozie Augustine
Yüksek Lisans Derecesi, Sürdürülebilir Çevre ve Enerji Sistemleri Programı
Tez Yöneticisi: Assist. Prof. Dr. Ali Atashbar Orang
Ortak Tez Yöneticisi: Assoc. Prof. Dr.Elif Oğuz

Kasim 2022, 61 sayfa

CO_2 gibi sera gazlarını azaltmaya yönelik sürekli artan küresel ilgi için yenilenebilir enerji kaynakları mükemmel birer alternatif olarak karşımıza çıkmaktadır. Sadece üretim dönemlerinde sürdürülebilir bir seçenek olmakla kalmayıp, aynı zamanda özellikle geleneksel fosil yakıt kaynaklarına kıyasla düşük bir uygulama maliyetine sahip olmaları üreticiye büyük yarar sağlamaktadır. Hidrokinetik türbinler, düşük kurulum maliyetine ek olarak öngörülebilirlik, nispeten düşük görsel etki, yüksek enerji yoğunluğu, yüksek kapasite faktörü ve üretim kolaylığı gibi avantajlara sahiptir. Bu çalışma, düşük hızlarda çalışan Savonius Hidrokinetik türbinlerinin araştırılması ve optimizasyonuna odaklanmaktadır. Ticari çözücü olarak ANSYS CFX, kayan ağ tekniği ve uygun sınır koşulları kullanılarak geçici akış alanını simüle etmek için kullanılmıştır. Önemli kontrol parametreleri, en-boy oranını (AR), örtüşme oranını ve kanatların şeklini içermektedir. Sayısal kurulum, sonuçların literatürdeki mevcut çalışmaların sonuçlarıyla karşılaştırılmasıyla doğrulanmış olup, eliptik şekilli kanat tasarımı, geleneksel olana kıyasla daha yüksek pozitif tork ürettiği için bu çalışmada önerilmiştir. Mevcut literatüre dayalı olarak değiştirilmiş tasarım için optimal örtüşme oranı bulunurken, farklı AR değerleri test edilerek optimal AR tespit edilmiştir.

Anahtar Kelimeler: Yenilenebilir Enerji, Hidrokinetik Enerji Sistemleri, Hesaplamalı Akışkanlar Dinamiği (HAD), Savonius türbini, Sayısal Analiz

Dedicated to My Parents

ACKNOWLEDGMENTS

The author wishes to express his deepest gratitude to the thesis supervisor Assist. Prof. Dr. Ali Atasbhar Orang and co-supervisor Assoc. Prof. Dr. Elif Oguz for their immense contributions towards the completion of this thesis.

I would also like to thank my family, especially my parents, Mr. Christopher Offiah and Mrs. Nnenna Offiah for having supported me throughout my master's studies. I also extend my regards to my twin brother, Jideobi for the moral support he provided me with. In the same vein, I would also like to thank Syed Sameer Noman and Thraiye Seif Hemed for their friendship and support.

I am also greatly indebted to my friend and colleague Kaan, for his support and help in model creation in Autodesk Inventor.

TABLE OF CONTENTS

LIST OF TABLES

LIST OF FIGURES

LIST OF ABBREVIATIONS

CFD	Computational Fluid Dynamics
ESTR	Elliptical Savonius Turbine Rotor
FEA	Finite Element Analysis
HAWT	Horizontal Axis Wind Turbine
HKT	Hydrokinetic Turbine
PDE	Partial Differential Equations
RANS	Reynolds-averaged Navier-Stokes
SHT	Savonius Hydrokinetic Turbine
SIMPLE	Semi-Implicit Method for Pressure Linked Equations
SST	Shear stress transport model
SHT	Savonius Hydrokinetic Turbine
SWT	Savonius Wind Turbine
TSR	Tip Speed Ratio
UDF	User Defined Function
URANS	Unsteady Reynolds Average Navier-Stokes
VAHT	Vertical Axis Hydrokinetic Turbine
VAWT	Vertical Axis Wind Turbine

LIST OF SYMBOLS

SYMBOLS

σ	Solidity
a	Diameter of the central shaft [mm]
A_T	Projected area of turbine [mm^2]
A_d	Area of the test section or computational domain [mm^2]
AR	Aspect ratio
BR	Blockage ratio
BF	Blockage factor
C_p	Coefficient of performance
C_q	Torque coefficient
d_T/d_B	Diameter of blades [mm]
d_s	Diameter of rotor shaft [mm]
D_e	Diameter of stator region [mm]
D_{Top}	Diameter of Turbine [mm]
D_o	Diameter of end plates [mm]
e	Overlap distance [mm]
GA	Genetic Algorithm
GR	Gap Ratio
H_{TB}	Height of Turbine [mm]
k-ω	k omega

k-ε	k epsilon
N	Angular velocity (rpm)
$\emptyset$	Scalar quantity
O_d	Gap distance [mm]
OR	Overlap Ratio
ρ	Density of the fluid [kg/m^3]
P_{theory}	Theoretical power from the turbine [watts]
P_{turb}	Calculated power from the turbine [watts]
R	Radius of the turbine [mm]
Re	Reynolds Number
t	Thickness of blades [mm]
t_e	Thickness of endplate [mm]
T	Torque [N.m]
u_x	Velocity in x-direction
u_y	Velocity in y-direction
u_z	Velocity in z-direction
μ	Dynamic viscosity of the fluid [kg/ (m.s)]
$\boldsymbol{V}$	Velocity vector
v	Free stream velocity [ms^{-1}]
w	Angular Velocity [rad/s]
v_m	Blockage ratio modified velocity [ms^{-1}]
γ	Blockage ratio correction coefficient
λ	Tip speed ratio

CHAPTER 1

INTRODUCTION

People have always tried to extract energy from the natural resources provided by the environment. The hydro energy option for extracting energy has always proved efficient in this regard. Hydrokinetic turbines in this case are much cheaper to deploy than hydro dams. The geometric parameters of these hydrokinetic turbines play a crucial role in how much energy these turbines can produce. Hence, it has also become increasingly important with time to optimize the designs of these hydrokinetic turbines to efficiently extract energy.

In this thesis, a Savonius turbine is modified for a low-speed water flow of 0.5 m/s. The constant parameter used in this case is the aforementioned inlet or incoming velocity to the computational domain. Hossein et al [1] defined low-speed flow for Savonius Hydrokinetic turbines to be 0.48m/s . In this thesis, however low speed flow will be considered as 0.5m/s. This work contributes to the existing literature by proposing a new blade design that will have a higher coefficient of performance than the conventional design. The aspect ratio, overlap ratio and the blade shape are the design parameters that will be considered. A sustainability assessment is also made considering the impact of hydrokinetic turbines.

The Motivation for this study will be briefly explained in detail at the beginning of this chapter. A summary of the brief history of the trends, development, and deployment of hydrokinetic turbines is given in the next section. The objective and scope of this body of work will be given at the end of this chapter.

1.1 Motivation

In a bid to aid the transition to renewable and sustainable energy sources, hydrokinetic turbines (HKTs) have been one of the energy alternatives that have been adopted [2]. The relative ease of manufacturing HKTs was one of the motivations for researchers in this field to investigate and develop new HKT systems. Hence, over the years, many research institutes, governmental bodies, and companies have dedicated efforts to research and develop efficient hydrokinetic energy systems. Due to its ready availability, hydrokinetic energy solutions have also become a much more explored alternative, compared to other energy sources. Like its wind counterpart which is a natural resource, water is easily available and can be obtained from streams, oceans, and rivers. Energy from these water bodies can be extracted by harnessing the power of water canals and tidal channels. Compared to wind turbines, there is no need for rotor adjustment in hydrokinetic turbines [3], which makes their operation relatively quieter. Also, they contribute relatively less load to their supporting structures.

Savonius Hydrokinetic Turbines (SHTs) are relatively easier to control as there is no need for adjustment to incoming water flow. These aforementioned characteristics also enable Savonius turbines to be easily accessible in rural areas and communities where access to grid-generated electricity is restricted or impossible. SHTs fall under the category of Vertical Axis Wind Turbines (VAWTs). VAWTs usually have two categories, namely; the drag type Savonius rotors and the Darrieus type rotors. Both of which are known to have low self-starting torque. This property of VAWTs makes them a sometimes preferred alternative to Horizontal Axis Wind Turbines (HAWTs), since they can be used to generate power at relatively lower velocities. A downside though, is that conventional Savonius rotors are known to have the lowest C_p amongst other turbines as can be seen in Figure 1.1.

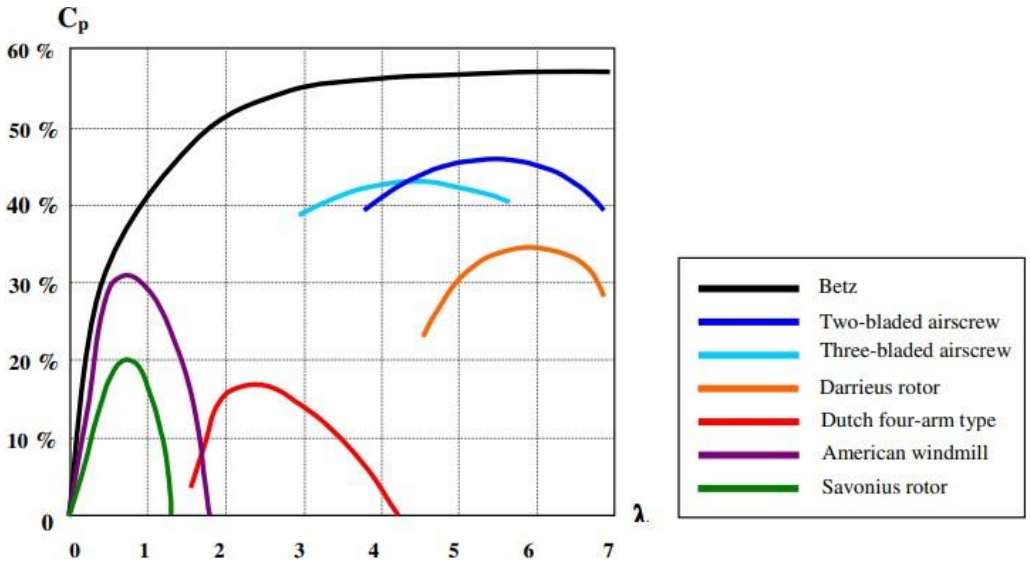

Figure 1.1:Comparison of coefficient of performance (C_p) for different wind turbine designs[4]

This is not to say that there have not been higher cases of C_p observed for different designs of turbines. Figure 1.1 just gives a generic C_p of conventional turbines based on numerous observed experiments. Even though Figure 1.1 represents wind rotors, there is no reason to assume that hydrokinetic rotors do not behave in a similar manner.

However, there have been studies that implemented modifications to the design of the conventional Savonius turbines for various geometries. These modifications have been known to improve power output. Such geometrical modifications whose variation has been found to significantly improve the performance of Savonius rotors include modifications to the following geometric properties; aspect ratio, gap ratio, overlap ratio, and blade shape. These aforementioned properties are discussed in detail in the methodology section. A major issue with the experiments and simulations that have been performed thus far is that most of them do not provide a general guide to account for various parameters in the design of Savonius Turbines. A design that works well within a certain range of incoming fluid velocity may fail for other ranges of fluid velocities.

According to Laws and Epps, the rated speeds at which simulations are done for hydrokinetic turbines to generate energy usually range from 1.75-2.25 m/s [4]. As a result of this, it is important to have a controlling parameter, which is kept constant in all design stages. For example, while, simulating the effects of the aspect ratio of the turbines on power production, parameters such as overlap ratio and gap ratio are kept constant. Simulations and experiments have mostly been carried out to account for a single parameter in all design stages to come up with a final design. Most researchers have solely studied the effects of aspect ratio variation, overlap ratio variation, and blade shape variation independently.

1.2 Brief History of the Savonius Design

Gupta [5] in his work gives a detailed historical information about the development of the wind turbine. As far back as 5000 BC, wind energy has been used to power the movement of boats on the sea. The designs were primarily structured to have a Horizontal axis. It was not until later in the 12^{th} century that, there was a record of vertical axis wind turbines referred to as the Persian vertical axis windmills. Much like the current Savonius-styled turbines, these earlier designs of VAWT operate using drag force, which ensures that the blades turn by a torque created by pressure difference. It was not until 1931 that Darrieus patented his design of the VAWT which operates using a lift-based principle [6]. As already mentioned previously, lift-based designs of VAWTs have been found to be more efficient than drag-based models. Since it is not within the scope of this thesis to investigate the former, discussions of the lift-based operation have been left out.

Sir Sigurd Savonius in his initial investigation into the operation of Savonius turbines in both wind tunnels and open conditions discovered that the maximum C_p was at 32% and 37% respectively[7] . Although there have been studies right from the 1920s when Sigurd Savonius Johannes [8] invented the design, most of the relevant studies which have focused on optimizing its energy production have occurred over the past four decades. The next section shall discuss the basic operating principles of the Savonius rotor and the relevant parameters which are considered in its design.

1.3 Savonius Rotor and Operation Mechanism

The Savonius Hydrokinetic turbines are designed to have a vertical axis about which they rotate. As can be seen from Figure 1.2, Savonius turbines fall into the category of cross-flow turbines which may also include tapered designs of the Savonius rotors. These cross-flow turbines also present an added advantage since they are less affected by surrounding debris that might be present in the sea.

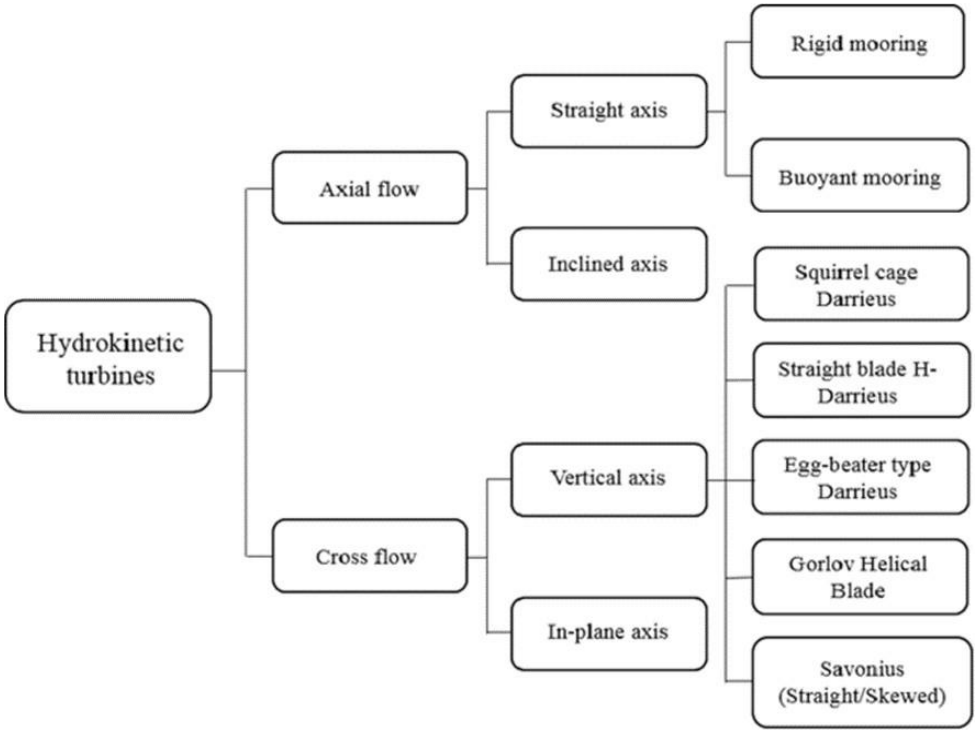

Figure 1.2 : Classification of Hydrokinetic Turbine rotors [4]

The Savonius rotor has an advancing and returning blade as part of its design. The advancing blade is the blade that is directly incident to the fluid flow direction and it generates positive torque, while the returning blade is the other blade that trails behind it and generates negative torque. The difference in these torque values is what enables the turbine to rotate.

The blade which has its shape open to incident flow is referred to as the concave blade, while the blade which has its shape seemingly trying to restrict the flow is referred to as the convex blade. Figure 1.3 shows a conventional Savonius rotor with its separation or gap distance, overlap, and axis of rotation. The axis of rotation also represents where the shaft of the rotor will be placed.

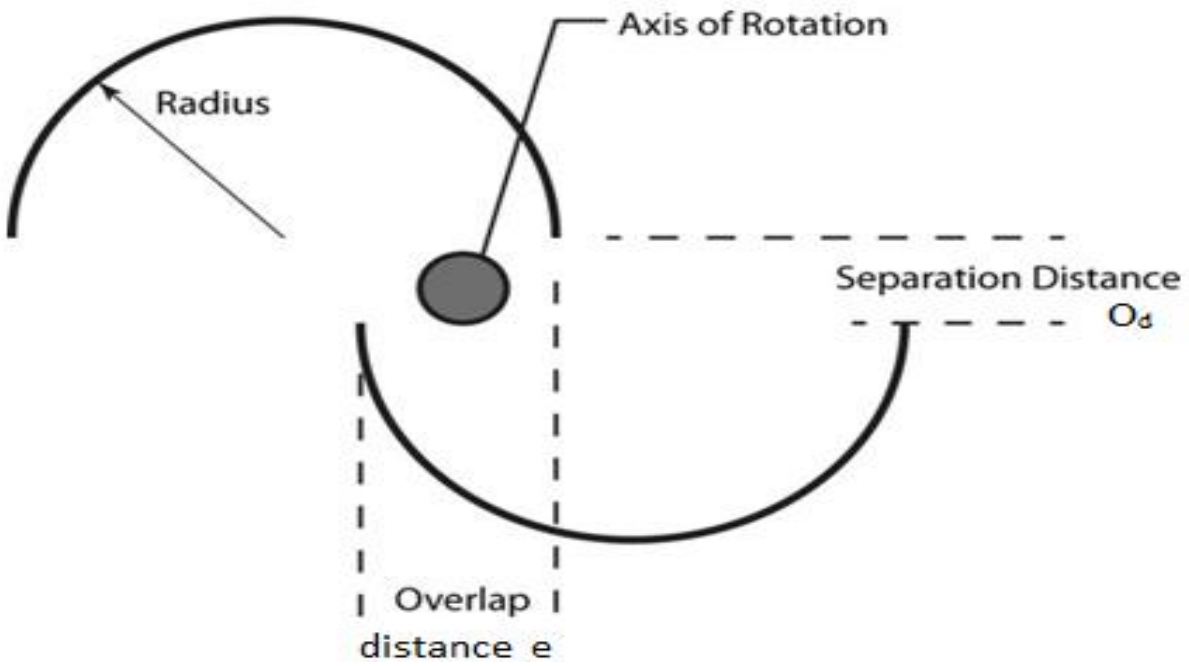

Figure 1.3: Top view of a conventional Savonius rotor showing vital parameters [8]

Figure 1.4 shows the flows grouped in numerals around the Savonius rotor. The flow labeled I and II create the drag force on the advancing and returning blades respectively.

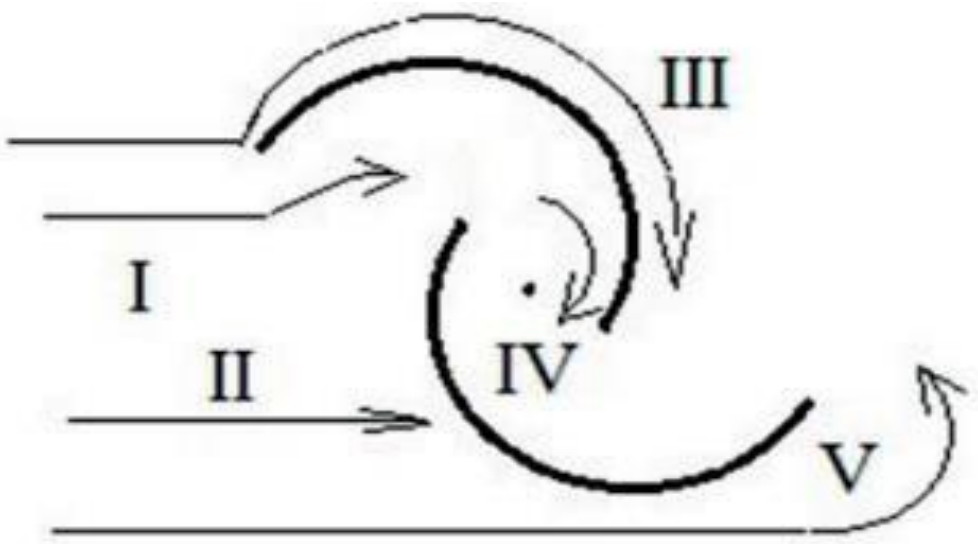

Figure 1.4: Major flow patterns on a Savonius Rotor [9]

Flow III which is the Coanda-like flow (a flow that follows the shape of the solid surface), is the flow responsible for bringing back the pressure on the concave side of the blade. The conventional Savonius turbine operates based on a drag mechanism. Recent studies have also shown that lift forces might also contribute to their torque rotation [10]. Figure 1.5 shows a schematic representation of a conventional Savonius turbine including various important design parameters.

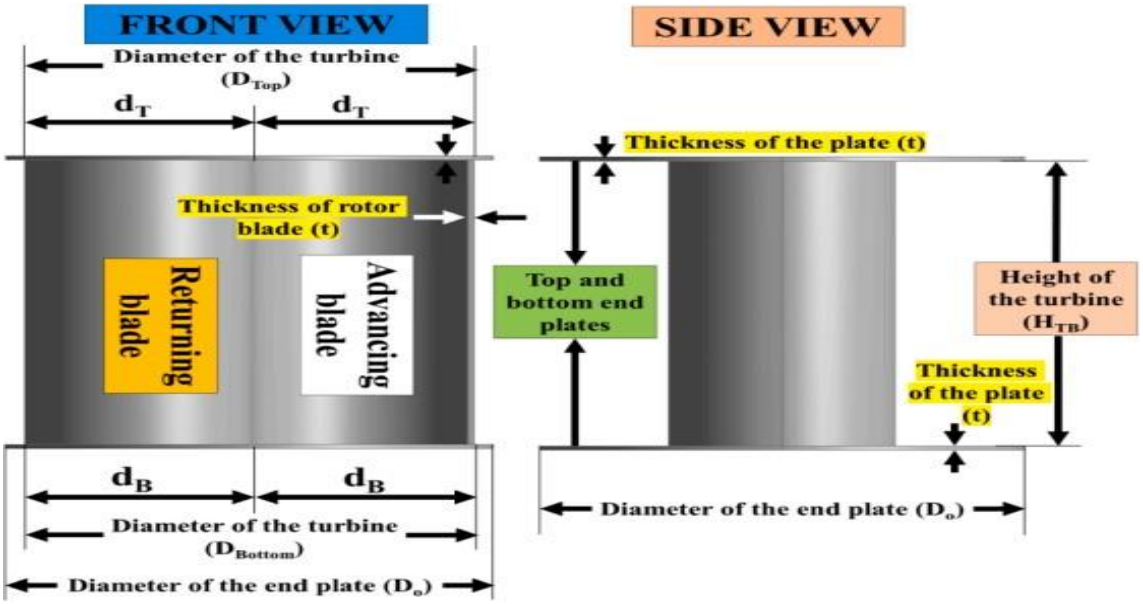

Figure 1.5:A 3-D model of the conventional Savonius Turbine with relevant geometric information [11]

This model also shows the end plates on the turbine. The end plates serve to stop the spillover of fluids over the turbine blades and consequently improve the efficiency of the turbine. They also add rigidity to the turbine rotor structure. In this study, d_T is equal to d_B. Hence, only the notation d_B will be used throughout this study.

1.4 Objective of the Thesis

The goal of this thesis is to optimize a Savonius Hydrokinetic turbine (SHT) design suited for low-speed operations. The flow velocity of 0.5m/s has been employed in this study. This study will consider the modification of three vital geometric parameters namely; the aspect ratio, overlap ratio, and blade shape of the turbine rotor. The Coefficient of performance (C_p) of the modified turbine will be compared with the C_p of the conventional design to see if it performs better. The effects of the torque coefficient C_q will also be discussed.

1.5 Scope of the Thesis

In order to extract energy from a hydrokinetic turbine, it is essential to design a turbine to meet the required energy demands. The parameters that are explored in this thesis work include the aspect ratio, overlap ratio, and blade shape. The modification involving the aspect ratio will first explore the conventional Savonius rotor design with a fixed overlap and gap ratio.

Furthermore, the aforementioned optimized turbine will be compared to the conventional design to show that they perform better than it. Unlike most of the work carried out in the literature, there was no experimental analysis to validate the results obtained by numerical simulation. Hence a number of techniques have been employed in this study to ensure that the work is as accurate as possible.

In the current literature, it is widely reported that the use of endplates significantly improves the value of the C_p and hence should be considered in the simulations. Nonetheless, the preliminary simulations in this thesis did not consider the operations of these turbines with end plates. This is because of Fujisawa's recommendation [12] which has been adopted by most researchers. Fujisawa concluded that the optimum diameter for the end plate (D_o) should be 1.1 D_{Top} where D_{Top} is the diameter of the turbine. In this study, the number of simulations run has been reduced based on the recommendations of researchers in the field. In the same vein, some of the simulations are carried out using a two-dimensional model. Even though 2-d models do not exactly represent the turbulent nature of the 3-d models, the C_p and C_q data obtained from 2-d models agree well with experimentally verified data [13].Also, the application of mesh-grid independence and the blockage factor (which is a function of the computational domain) in the results of C_p has also served to keep the results within the expected range.

Finally, for the final design, its operation has been studied a bit more in detail by exploring its power production over varying Tip Speed Ratios (TSRs) to get an idea of how much power is produced from the turbine rotor.

1.6 Thesis Overview

In Chapter 1, the basic information regarding this thesis and a brief history of the Savonius turbine is given. Chapter 2 summarizes the literature review of the relevant research works that have been carried out related to this thesis. In chapter 3, the basic fluid-related concepts and detailed information about the methodology applied in this study are given. In chapter 4, the computational fluid dynamics results and discussions are discussed. Also, the chapter includes the relevant assumptions, results, and discussions. Chapter 5, includes discussions about the sustainability impact of the final design. Finally, chapter 6, the concluding chapter summarizes the results obtained in this study. It also discusses future work that could be potentially be carried out.

CHAPTER 2

LITERATURE REVIEW

This section summarizes the research work that has been done in the literature which is relevant to this thesis. This section shall discuss the studies that have been carried out regarding the modification and optimization of Savonius turbines.

2.1 Effect of Aspect Ratio

Mabrouki et al [14] carried out an experimental investigation regarding the aspect ratio for Savonius hydrokinetic turbines by studying a 2-bladed semicircular HKT. They tested two turbines of height, 100mm and 200 mm both of which have a diameter of 190 mm. The corresponding aspect ratios of the turbines were 0.53 and 1.06 respectively. They obtained a C_p value of 0.19 and 0.047 for each turbine respectively. The optimum C_p value was recorded at an angular speed of 685 rpm and a tip speed ratio corresponding to an inlet velocity of 3.027. Even though this indicates that the coefficient of performance decreased with an increase in the aspect ratio of the turbine, the test is not exactly relevant due to the lack of a wider range of aspect ratios to make such a conclusion.

According to Patel et al [15], the optimum *AR* value was 0.6 for an overlap ratio of 0.11. Their study also found that for increasing aspect ratios after 1.8, the C_p was mostly stagnant and unchanging. They tested turbines for aspect ratios that ranged from 0.211 to 0.637 in little increments. The values for the C_p obtained were corrected using the blockage factor which shall be discussed later on in this thesis work.

In a similar fashion, Roy [16] tested five different aspect ratios ranging from 0.6 to 1 in a low wind speed test facility, the wind velocities varied from 5 m/s to 10 m/s. The optimum Aspect ratio was found to be 0.8. It is important to note that in this experiment, instead of varying the height of the turbine, as most researchers did in the current literature, Roy and Saha varied the diameter of turbines to achieve the aforementioned aspect ratios. Also worthy of note is that even though the maximum power was obtained for an aspect ratio of 0.6, the maximum C_p was obtained for a different aspect ratio of 0.8.

Alexander and Holownia [17] carried out a series of wind tests on 2,3 and 4-bladed helical turbines respectively. The varying aspect ratios of these turbines were varied from 1.2 to 4.8. Their findings indicate that the highest C_p of 0.25 was attained for a 2-bladed helical turbine with an aspect ratio of 4.8. Their investigations also pointed out that there was a significant decrease in the efficiency of the turbines when the 3 and 4 bladed turbines were tested in the wind channels.

However, the findings obtained by Frederikus et al [18] seemed to directly contradict the findings by Alexander et al. Similar to Alexander et al, Frederikus et al conducted their experiments on 2,3, and 4-bladed turbines. The key difference in both experiments is that Frederikus performed the experiments on straight-bladed turbines. Also, the focus of Frederikus' research was on finding the optimum number of blades required to give the best C_p. Surprisingly, they found out that a 4-bladed turbine performed better at lower tip speed ratios (TSR) while the 3-bladed turbines performed better at higher TSR.

Ivo et al [19] applied a genetic algorithm (GA) method to evaluate the different 3-D models involving 2, 4, and 6 blades respectively. This algorithm helped them to improve an already existing model to achieve an optimum C_p of 0.32 at an AR of 1.5 and a C_p of 0.34 at an *AR* of 2.5. The turbulence model which they employed was the *K-SST* model for their problem.

2.2 Effect of Blade Shape and Arc-Angle

One of the important parameters that have influenced the performance of the Savonius Turbine is its blade-arc angle. This refers to the angle made by the edges of each blade with the geometric center of the blades. Mao and Tian [20] performed 2-d simulations for different blade angles of Savonius wind turbines using Ansys Fluent 13.0. The angles ranged from 150 degrees to 200 degrees in increments of 10 degrees. Their findings indicated that the blade arc angle of 160 degrees yielded a coefficient of performance of 0.2836 which was the highest C_p detected in their study.

Chan et al [21] employed a GA to optimize the blade shape of a Savonius wind turbine using CFD methods. The genetic algorithm generated several ***candidates*** that could possibly perform better than the conventional semicircular turbine rotor. By using a 2-d model of the turbine blade and also employing the SST *k-w* turbulence model, they were able to obtain an improved C_p of 0.2255 for the turbine at a TSR of 1.2. This is a 33% improvement from the conventional turbine at the same TSR.

In the same vein, Sutaji et al [22] experimentally tested an elliptical Savonius turbine rotor (ESTR) design to enhance the power generation of a Savonius hydrokinetic turbine. The number of blades used varied from 2,3 and 4 blades in each stage of the experiment. Their results indicate that the highest C_p of 0.25 was obtained for 3 blades at a TSR of 2.37.

Konrad et al [23] performed both a numerical and experimental study of a conventional, Bach-type, and an elliptical Savonius wind turbine respectively. Their findings indicate that the elliptical turbines have the highest C_p at lower TSRs up to a tip speed ratio of 0.5. After which the Bach-type performed better up to the highest TSR of 1.2. Meanwhile, the conventional turbine rotor performs better than both the Bach-type and elliptical rotor only after a TSR of 1.1.

Yuvisika et al [24] performed a numerical simulation using ANSYS CFX-19, to compare the coefficient of performance of a semicircular hydrokinetic turbine to that of an elliptical turbine. The elliptical turbine configurations that were employed in this study were from turbines of 2,3 and 4 blades. All the numerical simulations were made at an inlet velocity of 0.6 m/s.

The elliptical turbines with 3 blades performed best with a maximum C_p of 0.738 at a TSR of 1.069. This is almost a 44% increase in performance from a semi-circular design which has a maximum C_p of 0.513 at a TSR of 1.2.

Researchers such as Sanusi et al [25] explored the combination of elliptical and conventional rotor designs to achieve improved turbine rotor performance. They were able to obtain an 11% increase in the maximum C_p obtained for a combined Savonius Wind Turbine (SWT) at a TSR of 0.79 when compared to the conventional Savonius rotor. This C_p was also 5.5% better when compared to the elliptical design.

2.3 Effect of Overlap Ratio

Thiyagaraj et al [26] experimentally aimed to obtain the optimal number of blades and overlap ratio for a Savonius hydrokinetic turbine. The inlet velocity in their experiment was 0.8 m/s and they tested for 2,3,4,5 and 6-blade configurations in their work. These initial models were designed to have an overlap ratio of 0. Their findings indicate that the 2-bladed turbines performed the best with a C_p of 0.105. Subsequently, they varied the overlap ratio from 0 to 0.3 in increments of 0.1, for the 2-bladed turbine. The turbine with an overlap of 0.2 performed the best with a C_p of 0.14.

However, the work by Tania et al [27] suggests that the overlap ratio of 0.15 is best suited for wind speeds below 4m/s. In their work, which was done experimentally they varied the wind speeds from 1m/s to 7 m/s for overlap ratios of 0.15, 0.20, 0.25, and 0.30. The turbine with an overlap ratio of 0.15 performed relatively better than the other turbines at velocities less than 4 m/s and the turbine with the overlap ratio of 0.3 performed better than the other turbines at incoming wind velocities greater than 4 m/s.

Gallo et al [28] performed a numerical simulation on a split-batch type Savonius rotor to determine which geometric ratios will give the best performance. They employed the surface response methodology technique. The parameters that were employed in this study included the width, overlap eccentricity, and radius of the rotor blade.

The overlap ratios that were tested ranged from 0.15 to 0.3. The optimum overlap ratio was found to be 0.2145 which had a corresponding C_p of 0.2661.

From the aforementioned works above, it can be seen that the optimum overlap ratios were 0.2 and 0.2145 respectively for the conventional and Bach-type Savonius turbines respectively. However, Alom and Saha [29] conducted a numerical investigation using Ansys-Fluent to find out what the optimum overlap ratio would be for an elliptical design of a Savonius wind turbine. They tested a range of overlap ratios for an elliptical Savonius wind turbine with a section cut angle of 47.5 degrees. The overlap ratios tested were 0.00,0.10, 0.15, 0.20, 0.25 and 0.3. The optimum overlap ratio and C_p were 0.34 and 0.15 respectively at a TSR of 0.8.

2.4 Summary of Literature and Research Gaps

So far in the studies conducted in the literature, the focus has been mostly on finding the optimum C_p by varying a single geometric parameter (aspect ratio, overlap ratio, gap ratio, and blade shape). This study proceeds in a different way by combining two parameters in finding the optimum C_p and maintaining the optimum value according to the literature for the third parameter (overlap ratio). The two parameters which were varied were namely the aspect ratio and the shape of the blade. The overlap ratio is kept at a constant of 0.15 throughout the simulation based on the recommendations from the already discussed literature.

The effect of the aspect ratio on the performance of the conventional Savonius turbine has also been assumed to influence the performance of the modified turbine. Consequently, the optimum aspect ratio for the conventional turbine is assumed to also be the optimum aspect ratio for the modified turbine rotor. The current literature also shows that most of the optimization studies have mostly focused on Savonius wind turbines, hence this study which focuses on Savonius hydrokinetic turbine would be a valuable addition.

CHAPTER 3

METHODOLOGY

In this study, the turbines are fully immersed in water. This is because studies by Talukdar et al [30] have shown that fully immersed turbines have a significantly improved C_p than partially immersed turbines.

3.1 Savonius Turbine Parameters and Relevant Equations

As was earlier discussed, certain geometric parameters affect the performance of a Savonius turbine. The first one is the aspect ratio (AR) given by

$$AR = \frac{H_{TB}}{D_{Top}} \tag{3.1.1}$$

The overlap ratio is given by

$$OR = \frac{e}{d_B} \tag{3.1.2}$$

The gap ratio is given by

$$GR = \frac{O_d}{d_B} \tag{3.1.3}$$

The coefficient of performance C_p which is a critical measure of the performance of a turbine is given by

$$C_p = \frac{P_{turb}}{P_{theory}} \tag{3.1.4}$$

Where P_{theory} is the theoretical power for the turbine and is dependent on the geometry of the turbines. P_{theory} is given by

$$P_{theory} = \frac{1}{2}\rho A_T v^3 \tag{3.1.5a}$$

Where A_T, the projected area of the turbine is given by

$$A_T = H_{TB} D_{TB} \quad (3.1.6)$$

The P_{turb}, is also the power transmitted from the shaft to the generator. It is given by (3.1.5b).

$$P_{turb} = \frac{T\pi N}{30} \quad (3.1.5b)$$

Where N is the angular velocity computed in revolution per minute (rpm). In this thesis, the software, Ansys CFX is used to compute the P_{turb} for each time step in the simulation. *T*, the torque is calculated by Ansys CFX while N is given directly as a user input.

Another important parameter is the torque coefficient. In this study, the torque coefficient is considered which is given by

$$C_q = \frac{T}{\frac{1}{2}\rho A_T v^2 R} \quad (3.1.7)$$

The expression in the denominator represents the total torque developed in the flow while T, represents the generated torque during the flow.

In this thesis, the torque developed during the flow is computed by the software Ansys CFX. The torque, T is given by

$$T = RF \sin\theta \quad (3.1.8)$$

Where *R* is the radius of the turbine, F is the force generated by the fluid interaction with the turbine and theta is the angular distance between the force and the distance from the axis of rotation. The torque should also be considered during the design of the turbines since high fluctuations in torque can be detrimental to the lifespan of the turbine, eventually leading to the failure of the turbine [31]

The tip speed ratio (TSR) λ is given by

$$\lambda = \frac{wR}{v} \tag{3.1.9}$$

Where *w* is the angular velocity of the turbine in radians per second. The TSR of a Savonius rotor is a very vital parameter considered in making the choice of what shape of rotor to use, as Amiri et al indicate in their work [32]. Hence it is necessary to characterize a turbine by simulating it over varying tip speed ratios.

3.2 Governing Equations

Since this whole thesis deals with fluid flow, fluid dynamics concepts will be applied throughout this work. Fluid dynamics is a branch of fluid mechanics that describes the flow of fluids and the forces acting on them. Fluid dynamics is usually described by Navier-Stokes equations, which are a set of partial differential equations (PDEs) that allow us to understand the flow of incompressible fluids (in this case, water).

These PDEs are based on three laws of conservation namely; the conservation of mass, conservation of momentum, and the conservation of energy. The conservation of energy which is derived from the first law of thermodynamics is not described in this work since the fluid is considered to be of a constant density and unaffected by temperature. Given the complexity of these flows and the difficulty associated with finding an analytical solution, it is imperative to solve them numerically using computational fluid dynamics (CFD).

3.2.1 Conservation of mass

The conservation of mass also known as the continuity law describes that matter can neither be created nor destroyed. Hence, within an arbitrary control volume, the rate at which the mass changes is equal to the rate at which the mass is produced within that volume. This is described in differential form by

$$\frac{\partial \mathrm{u}}{\partial x}+\frac{\partial \mathrm{v}}{\partial y}+\frac{\partial \mathrm{w}}{\partial z}=0 \qquad (3.2.1)$$

Since we are not dealing with multiphase flows, (3.2.1) can also be expressed as

$$\frac{\partial \rho}{\partial \mathrm{t}}+\nabla.(\rho \mathbf{u})=0 \qquad (3.2.2)$$

For incompressible flows the first term in Equation (3.2.2) drops out leading to

$$\nabla.(\rho \mathbf{u})=0 \qquad (3.2.3)$$

3.2.2 Conservation of momentum

The conservation of momentum describes the rate at which the material volume changes. This is equal to the total force acting on the volume. Equations 3.2.4 a, b and c are the Navier stokes equations for incompressible flow.

$$\rho(\frac{\partial u_x}{\partial t}+u_x\frac{\partial u_x}{\partial x}+u_y\frac{\partial u_x}{\partial y}+u_z\frac{\partial u_x}{\partial z})=\frac{-\partial p}{\partial x}+\mu(\frac{\partial^2 u_x}{\partial x^2}+\frac{\partial^2 u_x}{\partial y^2}+\frac{\partial^2 u_x}{\partial z^2})+\rho \mathrm{g_x} \qquad (3.2.4a)$$

$$\rho(\frac{\partial u_y}{\partial t}+u_x\frac{\partial u_y}{\partial x}+u_y\frac{\partial u_y}{\partial y}+u_z\frac{\partial u_y}{\partial z})=\frac{-\partial p}{\partial y}+\mu(\frac{\partial^2 u_y}{\partial x^2}+\frac{\partial^2 u_y}{\partial y^2}+\frac{\partial^2 u_y}{\partial z^2})+\rho \mathrm{g_y} \qquad (3.2.4b)$$

$$\rho(\frac{\partial u_z}{\partial t}+u_x\frac{\partial u_z}{\partial x}+u_y\frac{\partial u_z}{\partial y}+u_z\frac{\partial u_z}{\partial z})=\frac{-\partial p}{\partial z}+\mu(\frac{\partial^2 u_z}{\partial x^2}+\frac{\partial^2 u_z}{\partial y^2}+\frac{\partial^2 u_z}{\partial z^2})+\rho \mathrm{g_z} \qquad (3.2.4c)$$

3.2.3 Turbulence Modelling

D_{Top}, the diameter of the turbine is taken to represent the characteristic length [33]. This is because the characteristic length for Savonius turbine application is taken along the length of a body over which the flow develops. Equation (3.2.5) gives the expression for the Reynolds number, a dimensionless parameter.

$$Re = \frac{\rho v D_{Top}}{\mu} \tag{3.2.5}$$

The Reynolds number is known to affect the performance of Savonius turbines [34]. These turbines generally perform better at high Reynolds number than they do at lower Reynolds number. For this study, the minimum diameter of the turbine that was used is 0.415 meters.

Hence, solving with (3.2.6), we obtain a Reynolds number of 2.64 x10^8. In the investigation of the helical Savonius turbines by Damak et al [35], the critical Reynolds number was 116,064. This number is far less than the Reynolds number in this problem. Hence we consider this problem as a turbulent flow problem. The Reynolds number is a dimensionless parameter that is used to determine whether a flow is laminar or turbulent. It is the ratio of inertial forces to viscous forces. It is given by Equation (3.2.5) where ρ is the density of the fluid, v is the velocity of the incoming flow and μ is the dynamic viscosity of the fluid.

As previously described, turbulence is defined when the Reynolds number exceeds a critical number depending on the application. Other properties that characterize a turbulent flow include non-linearity of the flow, vorticity, dissipation, and diffusivity. To solve the equations of the flow described by Turbulence models, a time-averaging method is used, which averages the Navier-Stokes equation to give the Reynolds Averaged Navier-Stokes equations (RANS).

However, even with these averaging equations, there exist some unknown terms referred to as Reynolds Stress Tensors.

The presence of these unknowns which are more than the number of equations available creates a closure problem. Therefore, there is a need to model these Reynolds Stress Tensors using information about the mean flow [28]. Hence the need for turbulence models.

There are two turbulence models that shall be used in this thesis namely; the standard k-epsilon (Standard k-ε) model and the shear stress transport k-omega (SST k-ω) model. These aforementioned models have been known to give acceptable results for Savonius rotor simulation [36].

3.3 Computational Fluid Dynamics Analysis

Since it is analytically difficult or impossible to solve the governing equations of fluid dynamics, it is imperative to employ the techniques of computational fluid dynamics (CFD). To ascertain the accuracy of the results obtained in this thesis, a number of steps have been employed to make sure that the results are within an acceptable range. These steps have been explained in this section. They include a mesh independence study, application of the blockage factor to the results obtained and finally monitoring the convergence criteria to ensure that it converges within an acceptable range.

3.3.1 Finite Volume Method

This is a numerical discretization method that is used to solve partial differential equations of conservation laws, especially in the area of fluid dynamics [37]. Just like the finite element method, the finite volume method can be applied to both structured and unstructured meshes. However, in addition to that, the finite volume method maintains local conservativeness in each cell of a mesh. This conservativeness is maintained in all control volumes of a specific problem. In this method, the partial differential equations written in the form of volume integrals and containing divergence terms are converted to surface integrals using the divergence theorem. The finite volume method is quite robust in the sense that it can be extended to include problems of varying levels of difficulty. This method also has a good approximation to results obtained from practical flow problems [38].

3.3.2 Ansys CFX Solver

Throughout this thesis, the packages, Ansys Fluent and Ansys CFX have been used from the workbench environment of the Ansys package. Although the two software could be used to solve computational fluid dynamic problems (CFD), the methods they employ to solve these problems vary from each other.

While CFX and Fluent use the finite volume method which discretizes the computational domain by dividing it into mesh cells, both solvers employ a different type of discretization. Fluent uses the cell-centered method, while CFX uses the vertex-centered method [39]. CFX basically uses the method of Rhie and Chow interpolation [40] together with the aforementioned vertex-centered method. Figure 3.1 shows the vertex-centered and right-centered cell structures.

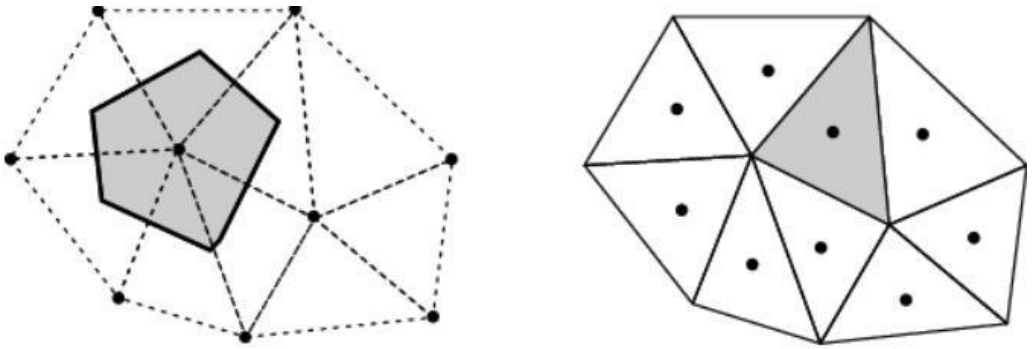

Figure 3.1:L-R Vertex-centered and Cell-centered Mesh [40].

Although 2-d simulations are applied in performing symmetrical modeling and using a simplified geometry which significantly reduces computational time, 3-D modeling of the turbines increases the computational time, but also improves the accuracy of the simulation [41]**.** As already mentioned, the CFD approach was used in this thesis. Numerous software such as Open Foam, SimScale, ParaView, and Ansys exist to solve various flow problems. However, Ansys has been known to give relatively better results for HKT simulation [42].

The software package Ansys Inc. CFX 22, is used in this thesis. The process of obtaining the results for a CFD simulation is done in three stages, namely; pre-processor, solver, and post-processor stages. Figure 3.2 summarizes this process.

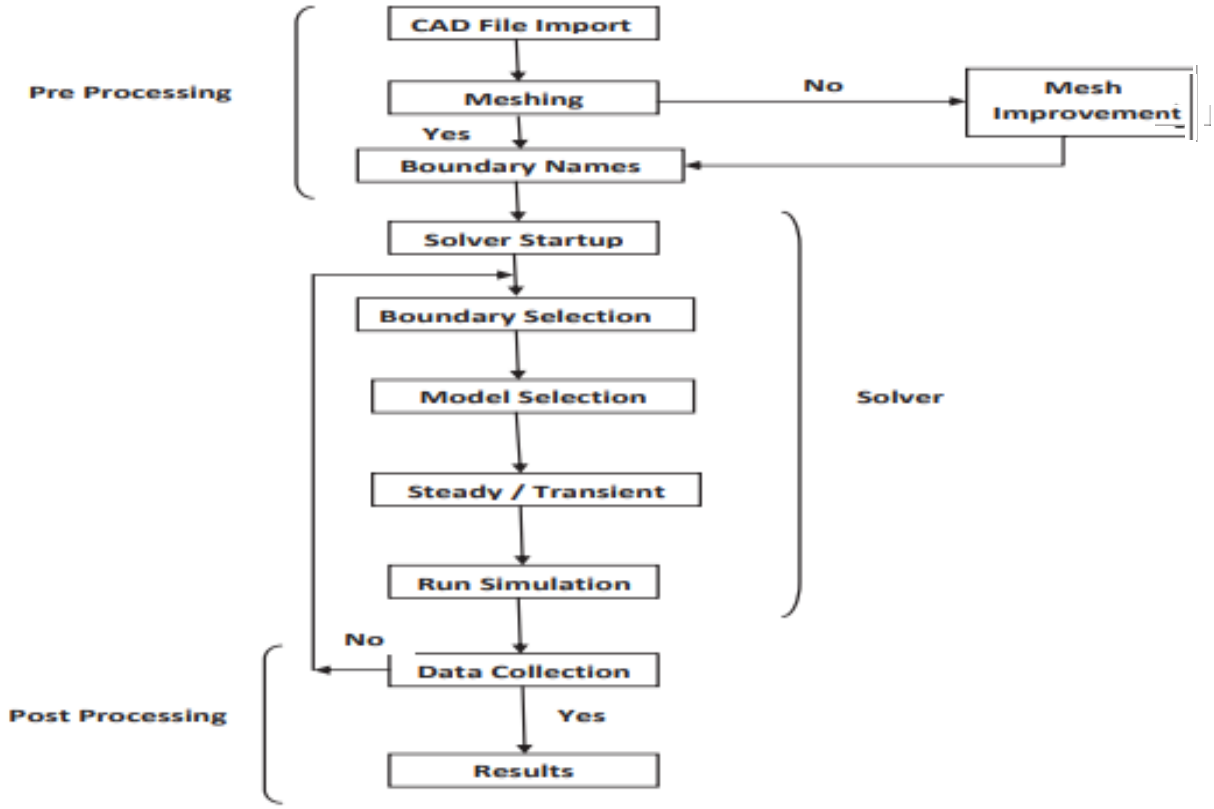

Figure 3.2: CFD modeling Methodology [43]

The geometries were created with the help of Autodesk Inventor. The meshing tool was used to mesh the imported geometry, after which the boundary names were assigned. The details of these boundary names are explained clearly in Chapter 4. Subsequently, the meshed geometry and computational domain are run to obtain the final results. Table 3.1 summarizes the solution method employed in this thesis.

Table 3.1: Solution Methods employed

Pressure-Velocity Coupling	
Scheme Used	SIMPLE- Semi-Implicit Method for Pressure Linked Equations
Discretization	
Gradient	Least Square Cell-Based
Pressure	Second Order Backward Euler
Momentum	Second Order Upwind
Turbulence Kinetic Energy	First Order Upwind
Residual Type	Root-mean square method (RMS)
Transient Scheme	Second-Order Backward Euler

The SIMPLE algorithm discretizes and solves the continuity and Navier-stokes equation in a semi-implicit manner [44]. It does this by using a relationship between velocity and pressure to establish a mass conservation and consequently obtain a pressure field. The flow properties for this problem are obtained from the solution to the URANS (Unsteady Reynolds Average Navier-Stokes). The solutions are obtained for each meshed cell in an iterative manner.

3.3.3 Mesh Independence Study

The mesh or grid independence study is used to determine the most suitable mesh for a given problem [45]. This is done by varying the size or type of mesh and monitoring a notable parameter until there is no notable changes in that parameter. Depending on the literature material studied, this method of mesh independency may also be referred to as sensitivity analysis. In essence, the idea is to see how the mesh parameters and variation affect the intended results. In this thesis, the sensitivity analysis is done initially for the simulations. The mesh independence study was done for the final design of the turbine in section 4.2.4, which included the combined blade model. In addition, the accuracy of the results obtained have been judged by observing two other parameters namely; the skewness of the mesh and the orthogonal quality of the mesh.

The Ansys guideline [46] suggests that that the maximum skewness of a 3-D mesh should be 0.9 and the average skewness of a mesh should not be more than 0.4. The guide also suggests a minimum orthogonal quality of 0.1.

3.3.4 Blockage factor

The computational domain is a salient parameter to consider when simulating fluid flow over bluff bodies. Results from the experiments that have been carried out, especially in wind-tunnel laboratories have been known to be considerably influenced by the size of the testing channel. This is because the narrower the size of the domain, the more fluid characteristics are influenced by Savonius rotors. The four walls around the Savonius rotor act as boundaries [47]. This effect is referred to as the blockage effect. Researchers have developed a correction factor based on physical experiments and numerical simulations to account for this. This correction factor is referred to as the Blockage factor. The blockage factor is dependent on the blockage ratio. The blockage ratio is given by

$$BR = \frac{A_T}{A_d} \tag{3.3.1}$$

where A_d is the area of the computational domain.

The Pope and Harper correlation [48] is given by Equations (3.3.2) and (3.3.3).

$$v_m = v(1 + \varepsilon_t) \tag{3.3.2}$$

Where v_m is the modified free stream velocity and ε_t is defined as

$$\varepsilon_t = \frac{BR}{4} \tag{3.3.3}$$

Dossena et al [49], suggested that the *BR* must be at least 0.1 for the BR to be considered in the calculation of C_p. Abdolrahim et al [50] also suggested that blockage ratios less than 0.05 could also be ignored. However, in this thesis. the blockage factor has been considered for all blockage ratios.

3.3.5 Convergence Criteria

Fluid dynamics deals with problems that are, for the most part innately unsteady phenomena. CFD

methods that are designed to tackle these problems are also subjected to these unstable phenomena, for example, turbulent behavior. Hence, it employs an iterative process to consequently attain a final solution or reach ***convergence***. The convergence criteria are used to show when the results have reached an acceptable solution.

It is important to note that convergence does not imply that an accurate solution has been found, instead it provides a limit within which the solution can be acceptable. Thus the convergence criteria limit varies for different problems. In this problem, residual values for the Root Mean Square Method is considered for convergence. Mohammed [9] suggested that even though the convergence of values below $1e^{-3}$ is weak, it is still sufficient for the Savonius rotor simulation. This thesis will consider the solutions to be sufficiently converged if the residual values fall below $1e^{-4}$. A typical convergence graph obtained in this study is shown in Figure 3.3. The graph shows the convergence of the x, y and z momentums.

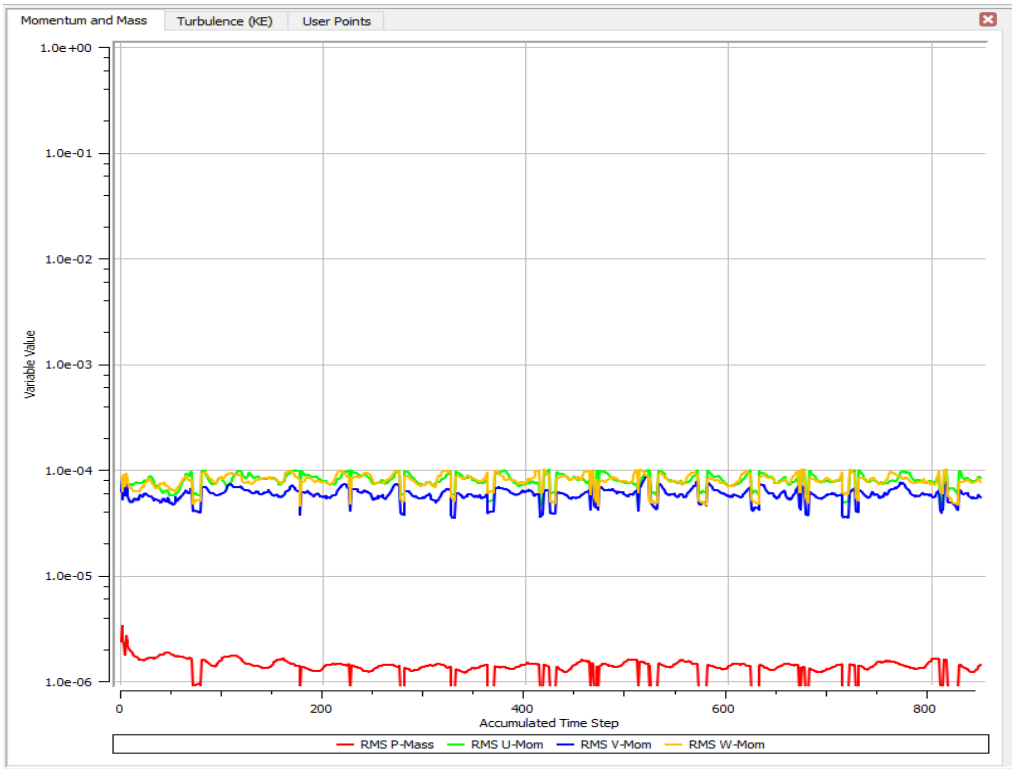

Figure 3.3: Residual Convergence plot in Ansys CFX.

In addition to the convergence criteria of $1e^{-4}$, an extra parameter such as inlet pressure is monitored. This parameter is monitored until there is significant changes in its value after successive iterations.

3.3.6 Flowchart for the Numerical Simulation

The flowchart for the general simulation of this thesis is presented in Figure 3.4. The study starts out with a set of simulations for the conventional turbines at an overlap ratio of 0.15. These set of simulations are carried out at varying aspect ratios from 0.5 to 2. The aspect ratio which gives the best performance for the turbine is detected. Consequently, the geometric height is chosen for the modified turbine blade based on this aspect ratio value. The simulation is carried out with the modified blade to ensure that the modified turbine shows an improved performance from the conventional turbine.

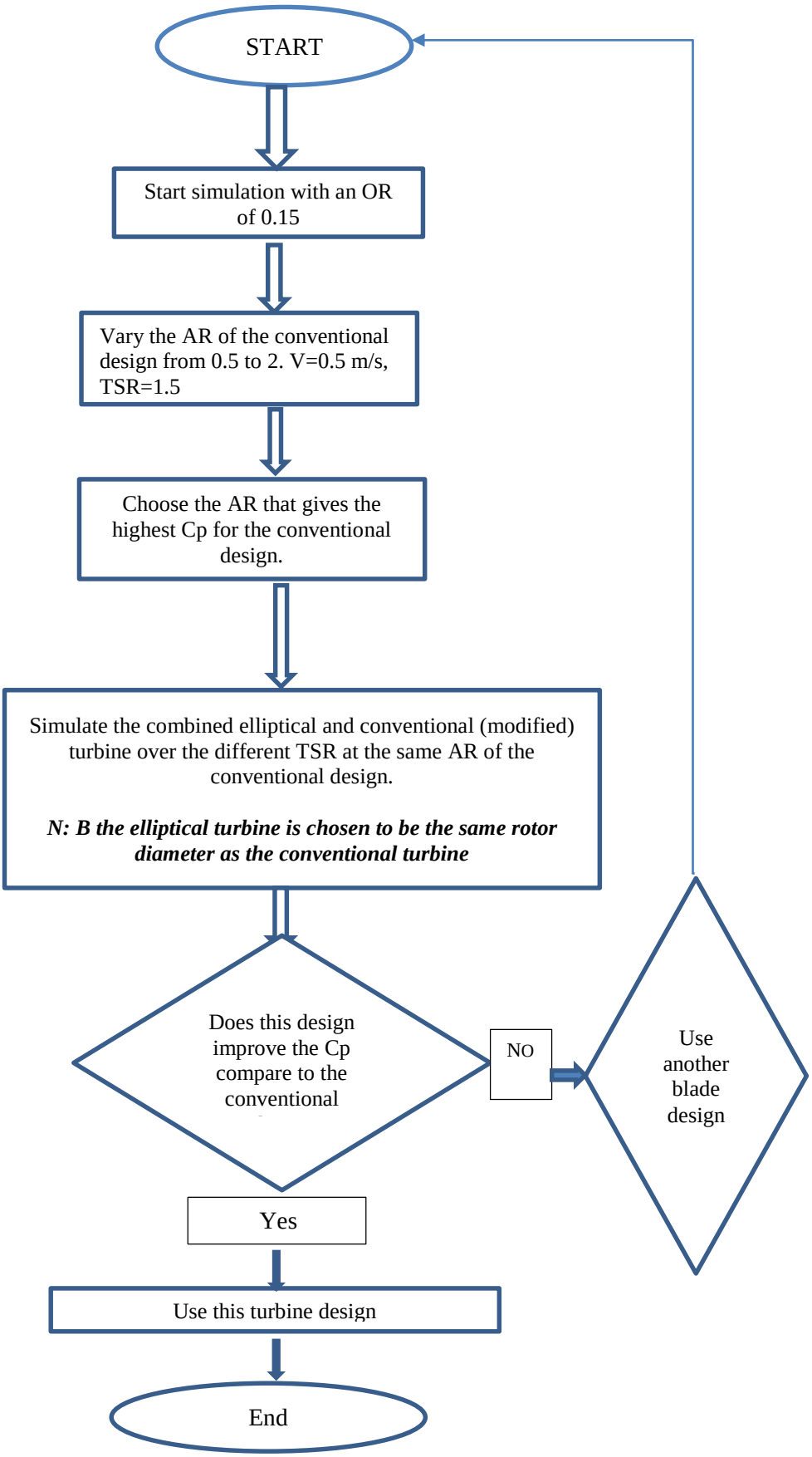

Figure 3.4:Flowchart for Numerical Simulation

CHAPTER 4

RESULTS AND DISCUSSION

The depth of the flowing water for the operating turbine is chosen as 2 meters. This is also the depth of the computational domain. In the first set of analyses, a conventional Savonius rotor is simulated for an inlet speed of $0.5ms^{-1}$ at a TSR of 1.5. The tip speed ratio (TSR) of the turbine is calculated from Equation (3.1.9). The relevance of the design parameters to be used will be classified from I to III, where I indicate most important and III indicates least important. The design parameters are classified below;

I Aspect Ratio

II Blade Arc Angle/Blade Shape

III Overlap Ratio

This chapter of the thesis starts out with a validation model that was carried out using the same parameters and conditions as proposed by the authors of the work.

4.1 Validation

To validate the current study one result is compared to the research work carried out by Shashikumar et al [11]. In their work, they investigated the effects of the conventional and tapered Savonius Turbines on an irrigation channel application. A description of the computational domain is given in Figure 4.1.

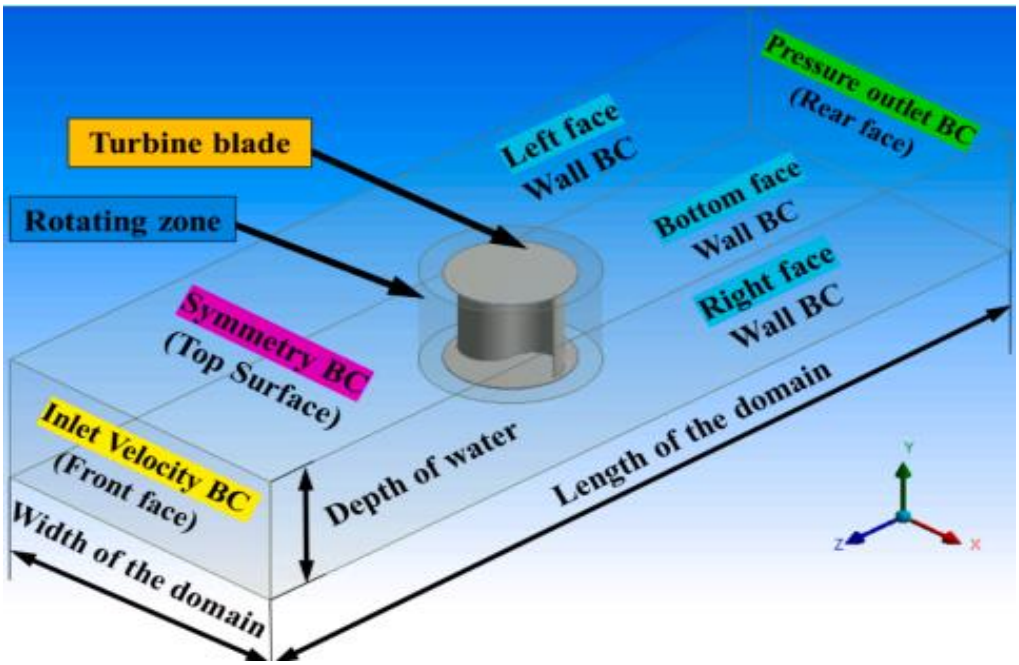

Figure 4.1: Computational domain for the validation model [11]

Using the same boundary conditions that were applied in this aforementioned work, a validation study is done to show how the C_p varies with respect to the TSR. They carried out the numerical simulation using Ansys Fluent. The inlet velocity was set at 0.5 m/s. This validation model was done for the variation of the conventional turbines' C_p with changing TSR using Ansys CFX. Figure 4.2 shows the validation study.

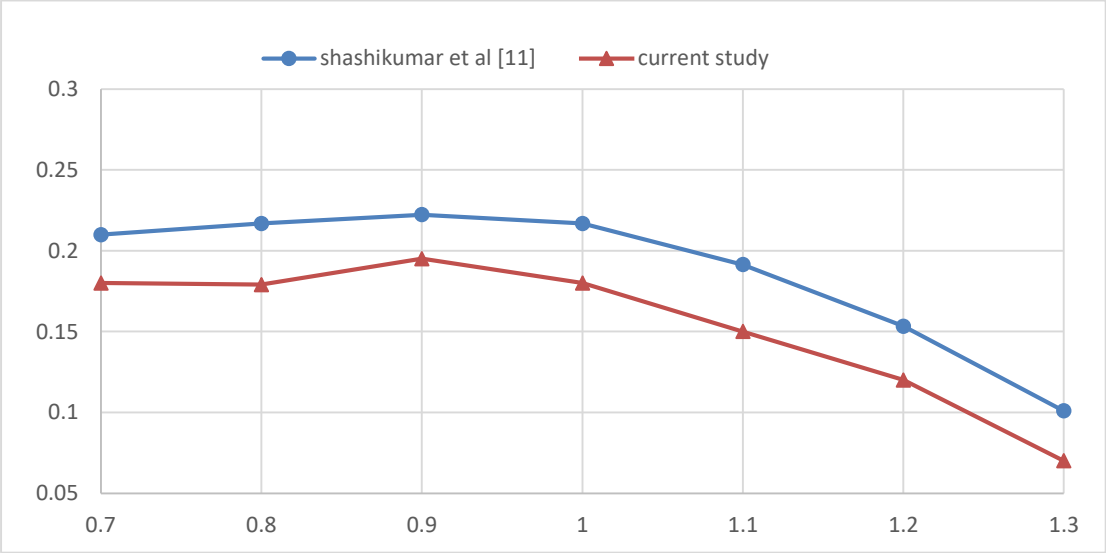

Figure 4.2: Validation for the variation of C_p with TSR

As can be seen from Figure 4.2, the validation follows the same trend as the current plot. There is however some error in the values obtained between the two plots as is summarized in Table 4.1.

Table 4.1: Percentage error between validation model and initial model for conventional Savonius rotor.

Tip Speed Ratios	Error %
0.7	14.25
0.8	17.45
0.9	12.25
1.0	16.99
1.1	21.64
1.2	21.70
1.3	30.61

The results obtained show that there is generally an increase in error between the plot of the current study and the validation plot as the tip speed ratios increase. The highest C_p of 0.22 obtained by Shashikumar et al [11] for the conventional turbine was at a TSR of 0.9. Similarly, the highest C_p obtained for the current study's plot is 0.195 at a TSR of also 0.9. The error margin at this TSR is 12.25%, which is also the lowest error margin that is detected. The results obtained for the current plot are at an acceptable value, hence the study can proceed.

4.2 Simulation for the Conventional blades

The first set of simulations aims to compare the coefficient of performance of various aspect ratios for the conventional design of the Savonius rotor. From the studies conducted by Alom and Saha [29], the optimal overlap ratio noticed across the literature was 0.15 for the conventional Savonius rotor.

Hence for this first set of simulations, all the turbine models have an overlap ratio of 0.15. The TSR used for this simulation is 1.5. This is because Mao and Tian [20] suggests that Savonius turbines generally have a higher coefficient of performance at higher TSRs.

4.2.1 Geometry for the Conventional Blades

This simulation is carried out to detect what the optimal aspect ratio will be. Table 4.2, presents the relevant geometric parameters that were used in this simulation. Where D_{Top} is the diameter of the turbine, d_s is the diameter of the shaft, H_{TB} is the height of the turbine, *AR* is the aspect ratio and *OR* is the overlap ratio.

Table 4.2: Geometrical Parameters for the Conventional Rotor Simulations

Design Case	d_s (mm)	D_{Top} (mm)	d_B (mm)	H_{TB} (mm)	*AR*	*OR*
Case 1	15	415	200	240	0.58	0.15
Case 2	15	415	200	335	0.80	0.15
Case 3	15	415	200	415	1.0	0.15
Case 4	15	415	200	625	1.5	0.15
Case 5	15	415	200	830	2	0.15

In this simulation, the computational domain which is a vital parameter in these simulations is set in such a way as to minimize blockage effects. Figure 4.3 shows the 3-d representation of the computational domain, with the turbine in green color.

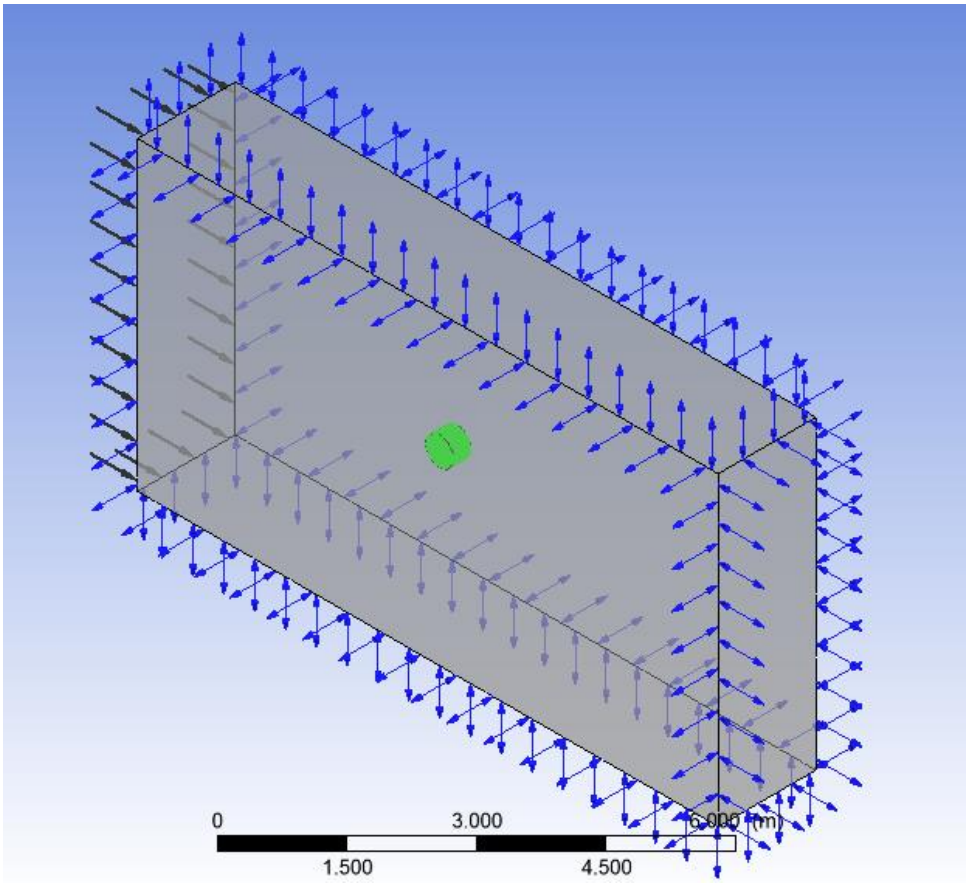

Figure 4.3: 3-d representation of the computational domain

In this thesis, the size of the computational domain is chosen as a factor of the diameter of the turbine. Figure 4.4 shows the required dimensions in 2-d. D1 indicated with the blue arrow represents the diameter of the rotor region. D1 is taken to be 1.12*D_{Top}. The rest of the region bounded by the rectangular region is referred to as the stator region. V3 is 5*D_{Top}, H2 is 11*D_{Top} while L11 is taken to be half of V3.

The distance between the inlet area of the computational domain (left side of the figure) to the center of the turbine is taken to be 3*D_{Top}.

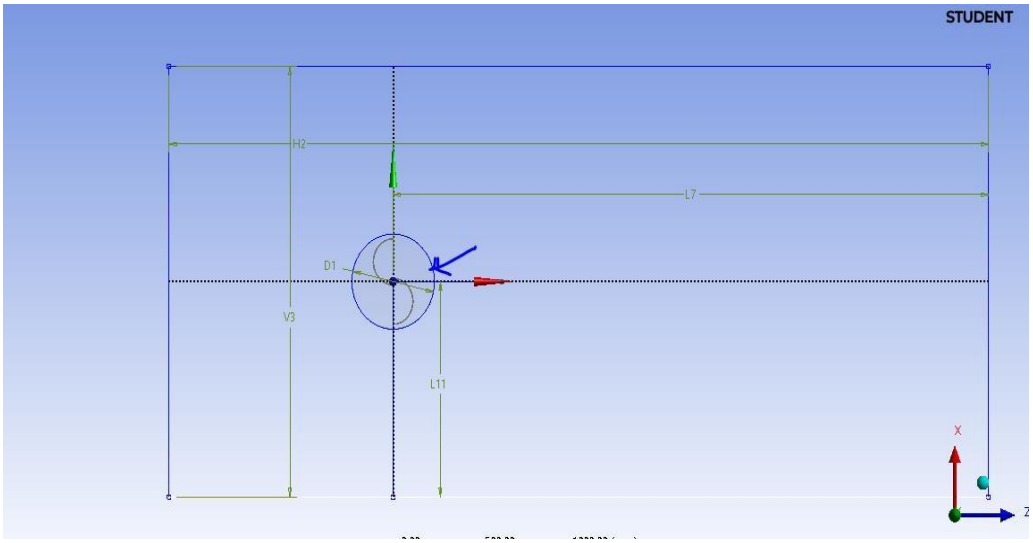

Figure 4.4: Dimensions for the Computational Domain of Conventional Savonius Rotor

The recommendation for distance from the inlet to the center of the turbine is based on the thesis work carried out by Chinchore [51] who proposed that the distance from the inlet to the center of the turbine should be at least 1.5 times the size of the diameter. The width of the domain is chosen based on the work by Gallo et al [28], who used a width that was 5 times the size of the turbine rotor.

Mo et al [52] conducted a study on the influence of domain size parameters on the performance of Savonius wind turbines. They indicated that for outlet distances (distance from the center of the turbine to the outlet region) greater than 5*D_{Top} and above, the values of C_p obtained did not change much. In this thesis, the outlet distance of 8*D_{Top} is used. In this thesis, these aforementioned dimensions as a function of the rotor diameter is used throughout.

Using the ***named selections*** feature of the Ansys ***Design Modeler***, the **inlet**, **outlet,** and **open** regions is assigned. The inlet region is the beginning of the computational domain which is closest to the turbine rotor.

The outlet region is directly at the far end, while the open region is the rest of the computational domain. Table 4.3 presents these dimensions that were used for the computational domain.

Table 4.3: Dimensions for the Computational Domain of the Conventional Turbine

Dimension Name	Notation	Size (mm)
Length	H2	4570
Breadth	V3	2080
Distance to Rotor center from inlet	L7	1245
Diameter of Stator region	D1	465
Depth	----	2000

4.2.2 Meshing

The meshing is done to separate the domain into smaller elements over which the flow equations described in section 3.2 are solved. A triangular mesh was used for the 2-D simulations while a tetrahedral mesh was used for the 3-D simulations. Figure 4.5 shows the tetrahedral mesh of the applied on the turbine blade and rotor region.

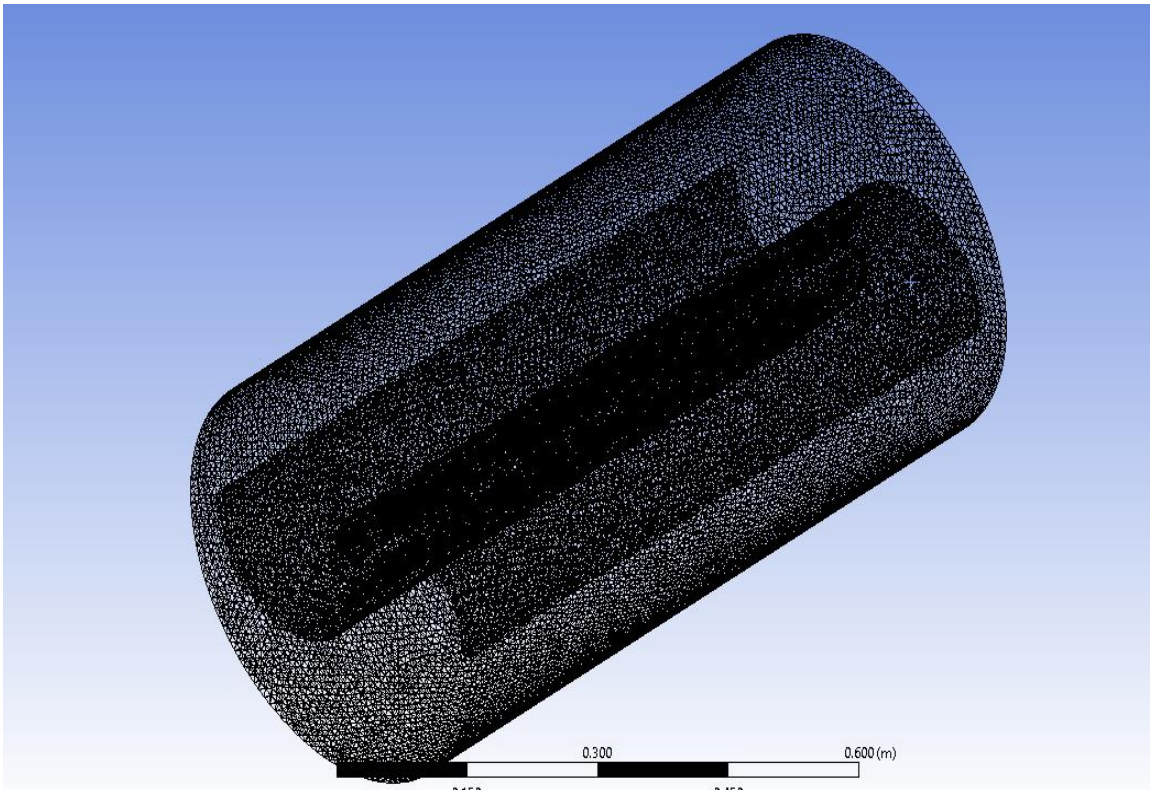

Figure 4.5: Tetrahedral meshing for the rotor region of the combined blade model.

4.2.3 Case Set-up

After the intended geometry is drawn using the tools of Autodesk Inventor. The geometry is imported into Ansys and meshed appropriately. The setup, which includes the boundary conditions is assigned to the computational domain.

There are two techniques that could be used during the simulation. They are the sliding mesh and dynamic mesh techniques. The ***sliding mesh*** allows the user to input a constant angular velocity for the bluff body (Savonius turbine). It creates two separate cell zones. The first one contains the cylindrical body that bounds the turbine. While the second one contains the remaining volume. This technique monitors time interactions between these cell zones to produce results. The sliding mesh technique also capture the effects of the rotational motion of the turbine. The dynamic mesh however, allows a new angular velocity to be calculated in each time step of the simulation. This value for angular velocity is calculated based on the present viscous forces of pressure acting on the flow regions.

This simulation is set as an Unsteady ***Transient*** simulation to account for fluid behavior over a period of time. Since we are dealing with low speed incompressible fluid the solver is set to a ***pressure-based*** solver. The gravity settings were not employed. Figure 4.6 shows the computational domain employed in this thesis, with the inlet, outlet, stator and rotor regions.

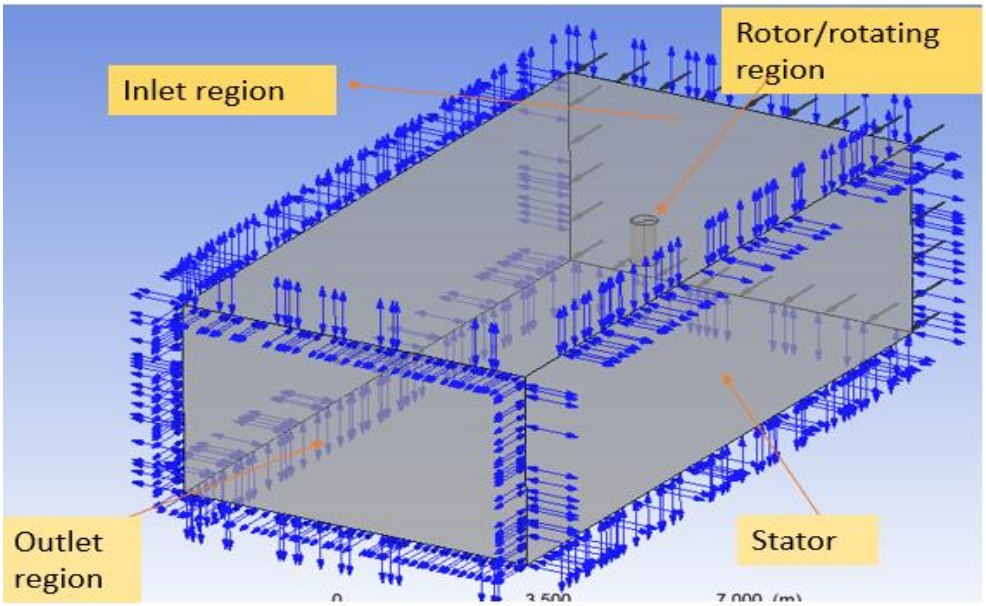

Figure 4.6: 3-D Computational domain for the simulation

Table 4.4 shows the numerical boundary conditions that were applied to the simulation flow problem.

Table 4.4: Boundary Conditions applied in the numerical simulation

Location On Computational Domain	Boundary Type	Boundary Conditions
Front face	Velocity Inlet	0.5 m/s
Back face	Opening	0 Pa gauge pressure
Left face	Opening	
Right face	Opening	
Bottom face	Opening	
Top face	Symmetry	
Savonius blade	Wall (No-slip)	Angular velocity is applied to the rotor region for varying TSR

4.2.4 Conventional Blade

Figures 4.7 and 4.9 describe the results of the C_p and C_q values obtained for the conventional design across different aspect ratios. The AR of 2 gives the highest C_p. What is notable though about Figure 13 is that the AR of 1.5 gives a lower C_p value than that of AR of 1.

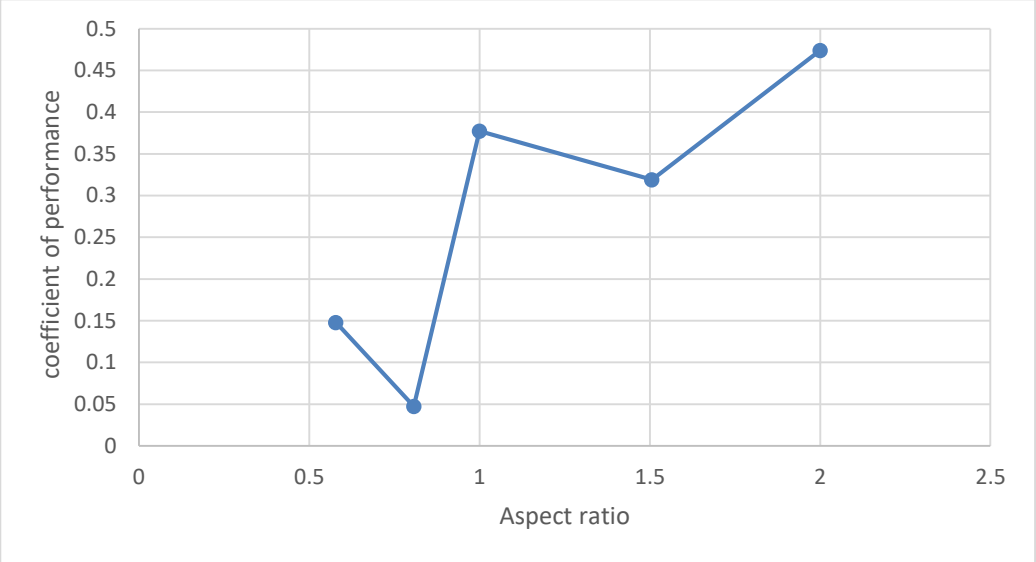

Figure 4.7: Power Coefficient Variation with respect to AR for the Conventional Savonius Design at 0.5 m/s and TSR of 1.5

Figure 4.9 shows the variation of the coefficient of performance in the stator region with respect to the change in the number of elements.

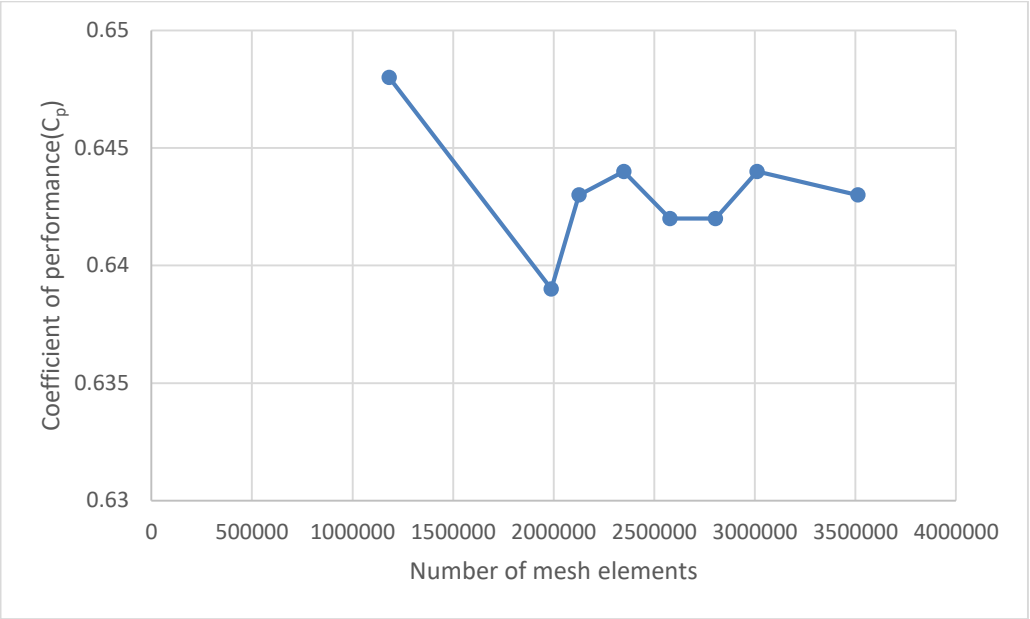

Figure 4.8: Mesh grid independency for AR=2, TSR=0.8

From Figure 4.8, it can be seen that the C_p for the modified turbine fluctuates about 0.644 as the number of elements in the stator region increases. Then number of elements used to achieve this is 3.5 million mesh elements

The Ansys CFX solver was set to 100-time steps for each period of revolution. Consequently, the power values were averaged in the 4th revolution (400-500 time steps), when the solution is judged to have converged. A similar procedure is applied to obtain the power and torque coefficients for the rest of the thesis.

The highest C_p for the conventional blade was obtained at an *AR* of 2, the combined modified blade turbine simulations will therefore be carried out at an *AR* of 2. The increase in C_p as the *AR* increases may be due to the blade tip losses which become less significant as the aspect ratio of the turbine increases [53] .

Figure 4.7, shows that as the aspect ratio of the turbine increases, the coefficient of the performance of the turbine does not necessarily increase as can be seen for *AR* values going from 0.5 to 0.8 and *AR* values going from 1 to 1.5. The maximum C_p of 0.47 was attained for the *AR* of 2. It is important to remember that the blockage factor discussed in section 3.3.4 was also applied to account for the effect of the size of the computational domain on the performance of the turbine. Figure 4.9 shows the variation of the Torque coefficient with the aspect ratio.

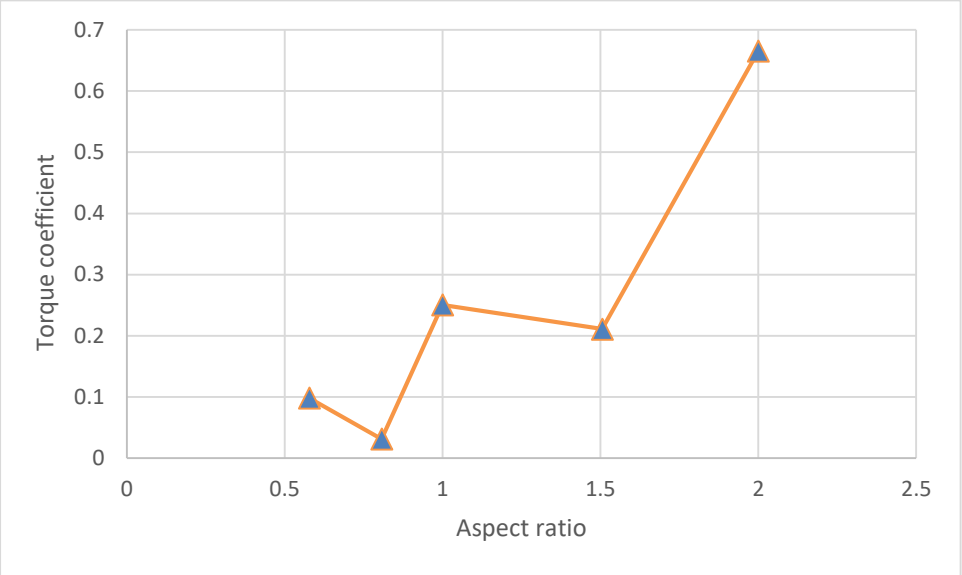

Figure 4.9: Torque Coefficient Variation with aspect ratio for the conventional Savonius blade turbine at inlet speed of 0.5m/s and TSR of 1.5

Figure 4.9, clearly shows that the maximum Torque coefficient of 0.67 also occurs at an aspect ratio of 0.2. Higher torque coefficients improve the performance of Savonius rotors by increasing the drag force on the advancing blades , which consequently improves the starting torque of the turbine [54].

4.2.5 Maximum Tip Speed Ratio

The method used here is the dynamic mesh method or flow-driven approach. For this blade design in question, the flow-driven approach is implemented. Zakaria and Ibrahim [55] suggest that this approach more clearly approximates the experimental results obtained.

As already explained, this method assumes that the turbine is in free flow as it would be if placed in water. The interaction of the forces in the fluid and the turbine enable the turbine to rotate at varying angular velocities throughout its operation as it would in real life. Using the dynamic mesh tools in Ansys fluent, the maximum tip speed ratio that was calculated was 1.5 for the conventional turbine.

4.3 Simulation for Modified Blades

The modified blade geometry and its CFD simulation are described in the following section. The conventional blades described in the previous section have been simulated at a tip speed ratio of 1.5. This is relatively higher than the tip speed ratio of 0.8 (the maximum tip speed ratio at which the modified blades were simulated). Although it seems out of place to establish a comparison between two turbines of different designs at two different tip speed ratios, various works in the literature have suggested that modified blades for SWT operate better than conventional blades at low Tip speed ratios [56] . This idea has been set out to be validated in this thesis.

4.3.1 Details of Geometry

Figure 4.10 shows the geometry with dimensions for the cross-section of the modified turbine rotor that was used in this thesis. The height of this turbine is 830 mm corresponding to an AR of 2.

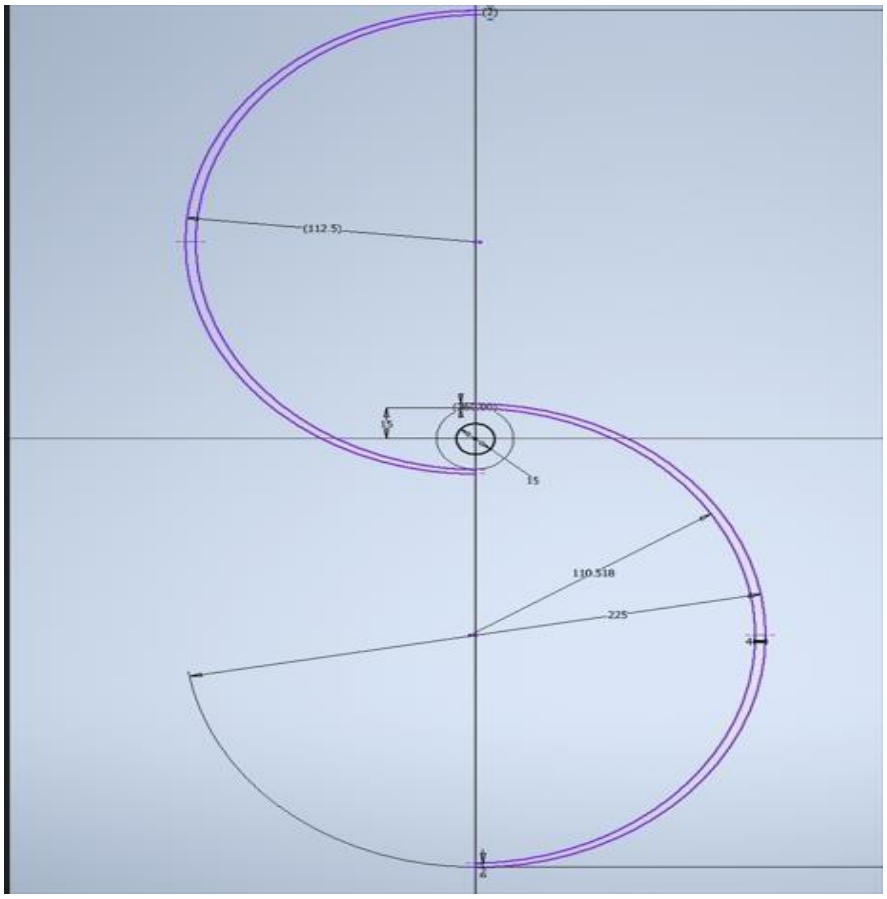

Figure 4.10: Geometry dimension for Modified (combined) blade

Hassan et al [57] compared three different models of a combined (elliptical and conventional Savonius turbine) with the conventional Savonius turbine. The three models included a semicircular turbine blade as the outer blade and an elliptical-shaped blade to be the inner blade. These models of the combined Savonius rotor performed better than the conventional turbine.

Out of the three models though, the model with the thinnest thickness performed best, with an increased C_p of 6.3% when compared with the two other models. Hassan et al proposed that this could be because such a design significantly improves the positive torque on the advancing blade and the negative torque on the returning blade. This difference in these moment values consequently improves the performance of the turbine.

In this work, a similar design is adopted, where outer blades are chosen to be the regular semi-circular conventional design and the inner blades are elliptical. In order to establish a basis of comparison, the total diameter of the modified rotor has been kept to be the same diameter as the conventional design. The overlap ratio of 0.15 has also remained unchanged. However, because of the inner elliptical blades, the overall thickness of the blades is made to vary between 0 to 6mm. Table 4.5 shows the variation of the mesh skewness as the number of elements and consequently, the number of nodes increased. These values agree well with the recommendations mentioned in section 3.3.1, which suggest that the maximum skewness should not be more than 0.9.

Table 4.5: Mesh Skewness details for the first four Simulations for Modified Blade at AR=2, TSR=0.8

	Rotor			Stator		
	Min.	Avg.	Max.	Min	Avg.	Max.
First Simulation	0.26935	0.76913	0.99364	9.763e-005	0.2219	0.74907
Second Simulation	5.04e-008	0.22306	0.74758	4.438e-005	0.21823	0.74856
Third Simulation	6.6119e-007	0.22215	0.74846	1.8553e-004	0.22033	0.74958
Fourth Simulation	2.2262e-008	0.21971	0.79272	2.5018e-006	0.21931	0.7502

Table 4.6 presents the mesh orthogonal quality for the first four simulations in the thesis for the modified blade turbine at TSR of 0.8. In the same vein, these values agree well with the recommendation that the minimum mesh orthogonal quality should be 0.1.

Table 4.6:Mesh Orthogonal quality details for the first four simulations for Modified Blade at AR=2, TSR=0.8.

	Rotor			Stator		
	Min.	Avg.	Max.	Min.	Avg.	Max.
First Simulation	2.133e-006	0.22954	0.73065	0.25093	0.77673	0.9947
Second Simulation	0.25242	0.77438	0.99632	0.25144	0.78053	0.99723
Third Simulation	0.25154	0.77612	0.99492	0.25042	0.77842	0.99547
Fourth Simulation	0.20728	0.77864	0.99763	0.2498	0.77949	0.99623

4.3.2 Modified Rotor over different tip speed ratios

The highest coefficient of performance of 2 is obtained at an aspect ratio of 2. Hence for the modified design, an aspect ratio of 2 is also chosen to run the simulations. As already discussed in 4.2.3, before a sliding mesh technique is applied, it is important to do dynamic meshing. This helps to identify the realistic angular velocities that exist for a given flow velocity and turbine design. As can be seen from in Figure 4.12, there is an increase in the Coefficient of performance of the turbine as the tip speed ratio increases. Characterizing the turbine over different TSRs helps to understand the mode of operation of these turbines better and compare different models of turbines.

Figure 4.11 shows the maximum power outputs for the modified design. The maximum power that could be extracted from the turbine is determined to be 16 watts. This is just enough to power 2 LED light bulbs or a fluorescent light bulb. Even though this might not seem like a lot of power, it is worth noting that the manufacturing costs of a Savonius turbine are quite cheap and affordable.

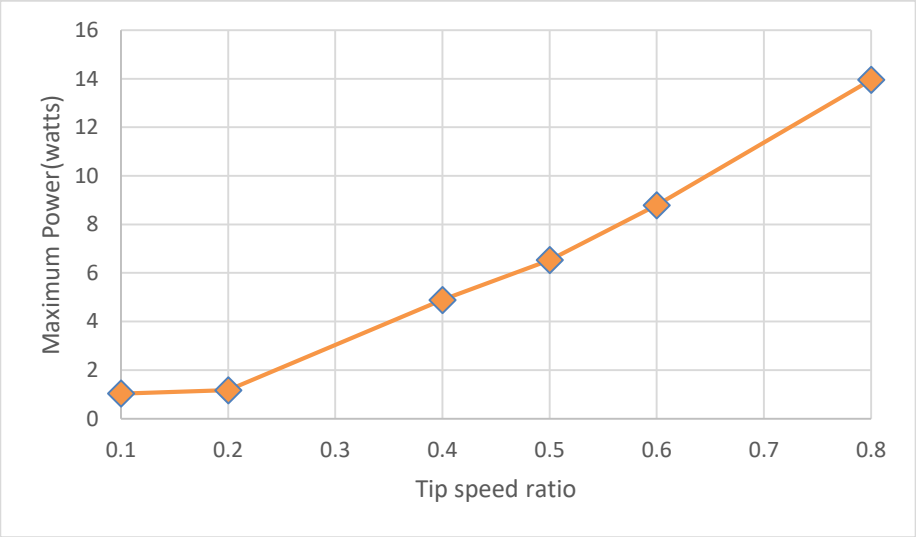

Figure 4.11: Power vs TSR for the modified Savonius turbine at AR = 2

To draw a comparison between the modified blade and the conventional blade, a coefficient of performance ($C_{p)}$ vs tip speed ratio (TSR) is plotted for the conventional blade at an aspect ratio of 2. Figure 4.12 shows the conventional blade and modified blade plotted on the same graph for a TSR range of 0.1 to 0.8.

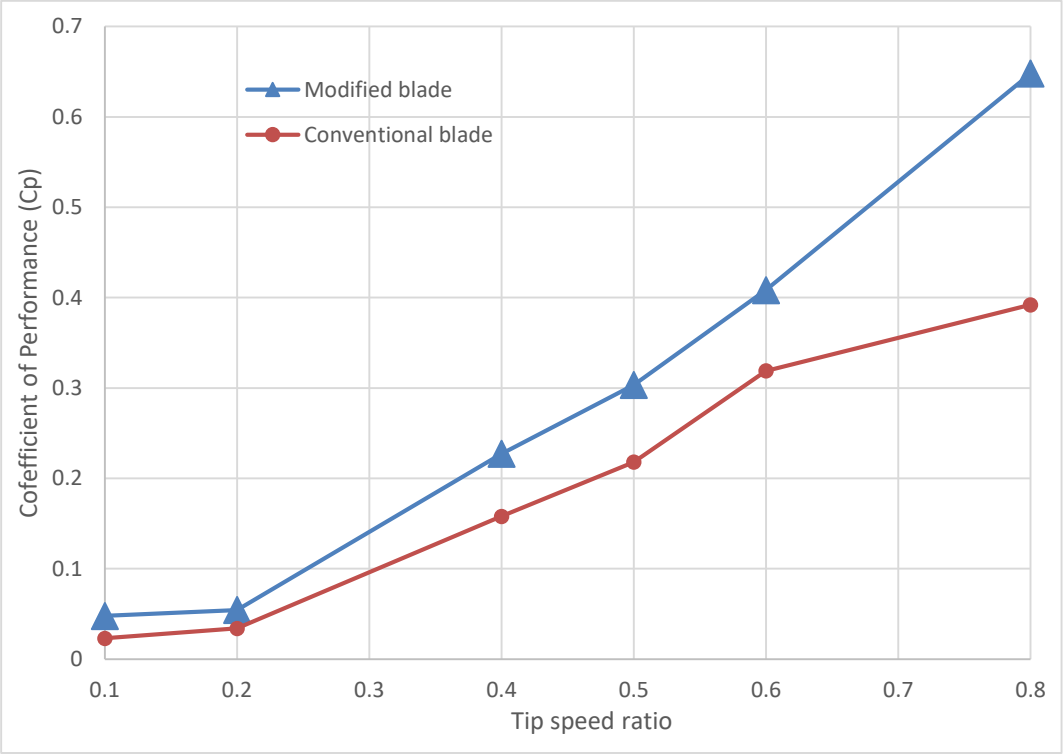

Figure 4.12: (a) C_p vs TSR for the conventional blade and modified (combined blade) blade

Much like the modified blade, the conventional blade also shows an increase in the coefficient of performance with an increase in tip speed ratio. However, the difference in C_p values between both blade models increases with an increase in Tip speed ratio, as can be seen at the tip speed ratio of 0.8, where the highest difference occurs.

As expected during the rotation of the blade, fluid forces are constantly acting on the blade to produce motion and consequently produce energy in the process. The motion of the blades in Figures 4.13 and 4.14 is counterclockwise. The incoming high velocity on the convex part of the advancing blade serves to create the rotational motion needed to move the blade, which in turn creates a high-pressure zone on its concave side. Figure 4.13 shows the velocity profile of the Savonius turbine after three revolutions of the blade. The difference in velocity magnitude in the two concave and convex regions), is what enables the blade to rotate.

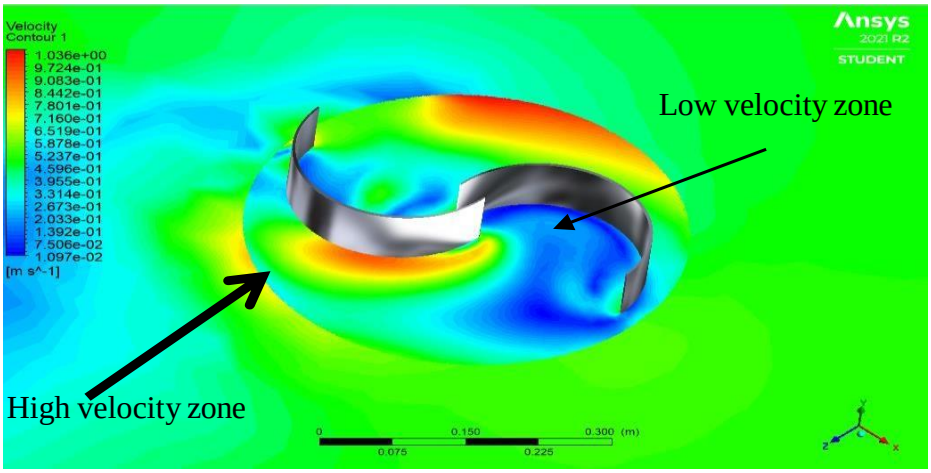

Figure 4.13: Velocity contour distribution around the modified turbine blade after 3 revolutions

Similarly, Figure 4.13 shows the pressure contour for the Savonius turbine after 3 revolutions. As can be seen from Figure 4.13, the lowest pressure zone is just closest to the convex side of the advancing turbine blade, while the highest pressure zone is on the concave side of the advancing blade. This large difference in pressure values for the blade enables the blade to rotate.

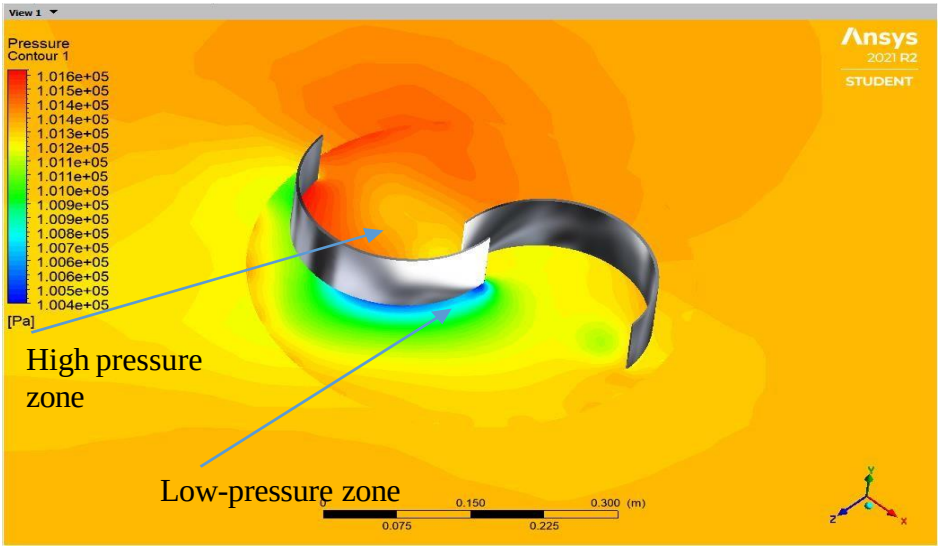

Figure 4.14: Pressure contour around the modified turbine blade after 3 revolutions

As expected, there could also be losses that occur in the operation of these turbines. These losses may be due to a number of reasons such as blade tip losses and cavitation. Cavitation in the turbine blades occur when the static pressure goes below the vapor pressure. This leads to flow separation and the formation of bubbles, that affect the performance of the turbine negatively [58]. However due to its low starting torque ability and consequently lower revolution per minute (rpm), the effect of cavitation on Savonius turbines (vertical axis wind turbines) is quite low when compared to the horizontal axis turbines .Hence, the effect of cavitation has not been studied in detail in this thesis [59].

CHAPTER 5

SUSTAINABILITY REVIEW

5.1 Sustainability Review

In these modern times, technology has advanced exponentially. Current turbines, due to their high potential, are a part of this advancement and have seen large scale development due to the amount of power that can be obtained from them. Hydrokinetic potential, whether it is in the form of ocean turbines or river turbines, has numerous advantages, the most significant being that it's energy output is highly more predictable than that of wind power. Additionally, once constructed and implemented, the minimum amount of maintenance is required with little to no engineering works required. Another benefit is that the turbines are hidden as they are totally submerged under water.

The new concept of hydrokinetic turbines is listed under goal number 7 in the sustainable development goals announced by the UN [60]. The 17 SDGs aim to establish a common framework for the policy and development agenda across the 193 UN member states, looking towards the year 2030. It has a general focus on hydropower, where if it is utilized in an efficient manner, it could provide for up to 16% of the world's energy and could bring energy services to billions of people. It provides numerous services such as but not limited to: freshwater management, climate mitigation, climate adaptation services, firm energy, energy storage and other ancillary services.
Hydrokinetic power, specifically, in relation to sustainable development has numerous positive impacts namely;

5.1.1 Effect on Climate

In the case of hydrokinetic power, the only time that greenhouse gases and emissions are produced is during the initial construction phase. Once built, and operational, it does not cause any release of harmful emissions to the environment. For sustainability purposes this is a big win and would be a highly preferred direction to proceed in.

5.1.2 Cycle of Operation

Hydrokinetic energy is a modern-day source of energy and not much information is available in the literature regarding its detailed life cycle analysis. However, it can be said that it has the same impacts to the environment that hydroelectric power and large onshore wind power had. Additionally, these are built over decades and require less amount of maintenance than normal dams that produce hydropower.

5.1.3 Ecological Impact

There is very little experimental data and results available in the case of hydrokinetic turbines and their effect on the ecosystems. There are various possible outcomes; firstly, the turbines could generate turbulence zones, which in turn could halt the development of aquatic life. Secondly, with the turbines generating kinetic energy, particles with nutrients could stay floating in the water, which could lead to a higher amount of plankton, and consequently, cause a rise in the fish population[61].

5.1.4 Health Concerns

Due to the nature of the location of hydrokinetic turbines, which is under the surface of the water, there is no noise pollution to the environment. In addition to that, efforts are made to ensure the recyclability of the materials used in turbine production. Hence, it could be said that it does not directly influence the quality of life in any negative way.

5.1.5 Area/Land Use

There are two parts to the turbine, one which is submerged under water and one that is above the surface for maintenance needs. Most energy structures such as windmills and transformers can be seen, however, in the case of the hydrokinetic turbines, the structure is less familiar to the eye and could be unsightly, especially in coastal areas where scenery is much appreciated [62].
Additionally, it has a negative effect on sports like swimming and tourism; since the area around the turbines would be dangerous, so would highly likely be out of service to the public. Paleo historical activities could also be greatly affected.

5.1.6 Local Economy

Another sustainable and social plus is that they can provide a significant amount of benefits such as power, electricity, and capital to the owner and installer of the turbines especially if they are from the host neighborhood. These turbines could also produce energy in localized areas that are cut off from the central grid. Additionally, maintenance is an easy aspect as well as inexpensive and provides for jobs locally.

5.1.7 Public Acceptance

Like every project and resource, hydrokinetic energy has its pros and cons. However, the advantages significantly outweigh the disadvantages. There is no noise pollution, a very low amount of environmental impact, barely any animal life is harmed by all the other positive aforementioned factors. For rural areas, the major challenge may be to get the dwellers of this aforementioned region to see the benefits of using hydrokinetic energy sources by outlining their benefits.

CHAPTER 6

CONCLUSION

In this thesis study, the modification of a VAHT, Savonius has been done to optimize the design for a low-speed flow of 0.5m/s. Previous researchers have carried out this modification process by focusing on a single parameter at a time. These parameters include the aspect ratio, overlap ratio, gap ratio and blade shape. Also these design modifications have been made for VAWT, and Savonius turbines. This thesis studies more than a single design parameter in the modification process for a Savonius hydrokinetic turbine. In this case, the aspect ratio (*AR*) and blade shape have been prioritized over other existing geometrical parameters. The focus has also been on a relatively lower velocity, compared to the ones obtained in the available literature.

The software that is used in this study include Ansys Fluent, and CFX, Microsoft Excel, and Autodesk Inventor. The CFD simulation of the conventional blades was used to determine which aspect ratio of blades will give a higher C_p. The final chosen *AR* of 2 is detected. This *AR* of 2 is used in the simulation of the modified blades. The modified blade is composed of both elliptical and conventional blade designs. To determine the operating TSR range dynamic mesh simulation is done to find the largest TSR corresponding to angular velocities with which the free-torque turbine could rotate. The results show that the C_p of the turbine at a TSR of 0.8 is 0.644. Subsequently, the coefficient of performance vs tip speed ratio of the conventional turbine and the modified turbine are plotted at an *AR* of 2, and a maximum TSR of 0.8. The results indicate that the modified turbine performs better than the conventional turbine over the range of tip speed ratios used (0.1-0.8).

The study of site-specific hydrokinetic turbines could also be explored in future studies. Site-specific turbine designs in this case refer to designs whose parameters are influenced by the environmental conditions of the deployment site. Further studies could be done on the development of Savonius hydrokinetic turbines with the assistance of established optimization techniques. Already in the current literature, a model known as the kriging model has been used together with computational fluid dynamics to build surrogate models. These surrogate models have increased data points that have been tested to obtain the maximum C_p values for Savonius turbines. Further work could be done

by applying the same surrogate model for the combined (conventional and elliptical design). Subsequently, optimization algorithms such as the Artificial Neural Networks (ANN) and genetic algorithms have been used to estimate the maximum C_p. Also, the literature has also been lacking in detailed structural analysis of not just the turbine itself but also the supporting structures of the turbine. Another future work in the area may be to study the operation of a group of these turbines in different configurations and studying their wake effects on each other and how they influence energy production in a specific site of interest.

REFERENCES

[1] H. Alizadeh, M. H. Jahangir, and R. Ghasempour, "CFD-based improvement of Savonius type hydrokinetic turbine using optimized barrier at the low-speed flows," *Ocean Eng.*, vol. 202, no. March, p. 107178, 2020, doi: 10.1016/j.oceaneng.2020.107178.

[2] N. D. Laws and B. P. Epps, "Hydrokinetic energy conversion: Technology, research, and outlook," *Renew. Sustain. Energy Rev.*, vol. 57, pp. 1245–1259, 2016, doi: 10.1016/j.rser.2015.12.189.

[3] S. Laín, L. T. Contreras, and O. López, "A review on computational fluid dynamics modeling and simulation of horizontal axis hydrokinetic turbines," *J. Brazilian Soc. Mech. Sci. Eng.*, vol. 41, no. 9, 2019, doi: 10.1007/s40430-019-1877-6.

[4] M. J. Khan, G. Bhuyan, M. T. Iqbal, and J. E. Quaicoe, "Hydrokinetic energy conversion systems and assessment of horizontal and vertical axis turbines for river and tidal applications: A technology status review," *Appl. Energy*, vol. 86, no. 10, pp. 1823–1835, 2009, doi: 10.1016/j.apenergy.2009.02.017.

[5] A. K. Gupta, "Efficient wind energy conversion: Evolution to modern design," *J. Energy Resour. Technol. Trans. ASME*, vol. 137, no. 5, 2015, doi: 10.1115/1.4030109.

[6] P. M. Kumar, K. Sivalingam, T. C. Lim, S. Ramakrishna, and H. Wei, "Review on the Evolution of Darrieus Vertical Axis Wind Turbine: Large Wind Turbines," *Clean Technol.*, vol. 1, no. 1, pp. 205–223, 2019, doi: 10.3390/cleantechnol1010014.

[7] S. J. Savonius and H. Finland, "The S-Rotor and Its Applications," *Mech. Eng.*, vol. 53, no. 5, pp. 331–338, 1931.

[8] J. P. Abraham, B. D. Plourde, G. S. Mowry, W. J. Minkowycz, and E. M. Sparrow, "Summary of Savonius wind turbine development and future applications for small-scale power generation," *J. Renew. Sustain. Energy*, vol. 4, no. 4, 2012, doi: 10.1063/1.4747822.

[9] M. H. A. Mohamed, "Design Optimization of Savonius and Wells Turbines," *Fac. Process Syst. Eng.*, vol. Doktoringe, p. 198, 2011.

[10] T. Zhou and D. Rempfer, "Numerical study of detailed flow field and performance of Savonius wind turbines," *Renew. Energy*, vol. 51, no. March 2013, pp. 373–381, 2013, doi: 10.1016/j.renene.2012.09.046.

[11] C. M. Shashikumar, H. Vijaykumar, and M. Vasudeva, "Numerical investigation of

conventional and tapered Savonius hydrokinetic turbines for low-velocity hydropower application in an irrigation channel," *Sustain. Energy Technol. Assessments*, vol. 43, no. March 2020, p. 100871, 2021, doi: 10.1016/j.seta.2020.100871.

[12] K. S. Jeon, J. I. Jeong, J. K. Pan, and K. W. Ryu, "Effects of end plates with various shapes and sizes on helical Savonius wind turbines," *Renew. Energy*, vol. 79, no. 1, pp. 167–176, 2015, doi: 10.1016/j.renene.2014.11.035.

[13] S. Mauro, S. Brusca, R. Lanzafame, and M. Messina, "CFD modeling of a ducted Savonius wind turbine for the evaluation of the blockage effects on rotor performance," *Renew. Energy*, vol. 141, pp. 28–39, 2019, doi: 10.1016/j.renene.2019.03.125.

[14] I. Mabrouki, Z. Driss, and M. S. Abid, "Experimental Investigation of the Height Effect of Water Savonius Rotors," *Int. J. Mech. Appl.*, vol. 4, no. 1, pp. 8–12, 2014, doi: 10.5923/j.mechanics.20140401.02.

[15] V. Patel, G. Bhat, T. I. Eldho, and S. V. Prabhu, "Influence of overlap ratio and aspect ratio on the performance of Savonius hydrokinetic turbine," *Int. J. Energy Res.*, vol. 41, no. 6, pp. 829–844, 2017, doi: 10.1002/er.3670.

[16] R. S. Sukanta , Ujjwal, "GTINDIA2013-3729," *Proc. ASME Gas Turbine India Conf. December 5-6*, vol. Conference, pp. 1–6, 2013.

[17] A. J. Alexander and B. P. Holownia, "Wind tunnel tests on a savonius rotor," *J. Wind Eng. Ind. Aerodyn.*, vol. 3, no. 4, pp. 343–351, Jan. 1978, doi: 10.1016/0167-6105(78)90037-5.

[18] F. Wenehenubun, A. Saputra, and H. Sutanto, "An experimental study on the performance of Savonius wind turbines related with the number of blades," *Energy Procedia*, vol. 68, pp. 297–304, 2015, doi: 10.1016/j.egypro.2015.03.259.

[19] I. Marinić-Kragić, D. Vučina, and Z. Milas, "Global optimization of Savonius-type vertical axis wind turbine with multiple circular-arc blades using validated 3D CFD model," *Energy*, vol. 241, 2022, doi: 10.1016/j.energy.2021.122841.

[20] Z. Mao and W. Tian, "Effect of the blade arc angle on the performance of a Savonius wind turbine," *Adv. Mech. Eng.*, vol. 7, no. 5, pp. 1–10, 2015, doi: 10.1177/1687814015584247.

[21] C. M. Chan, H. L. Bai, and D. Q. He, "Blade shape optimization of the Savonius wind turbine using a genetic algorithm," *Appl. Energy*, vol. 213, no. August 2017, pp. 148–157, 2018, doi: 10.1016/j.apenergy.2018.01.029.

[22] A. Sutaji, M. Yusvika, D. D. D. P. Tjahjana, and S. Hadi, "Application of Elliptical Blade

Shape to Enhance Power Generation of the Savonius Water Turbine," *IOP Conf. Ser. Mater. Sci. Eng.*, vol. 1096, no. 1, p. 012049, 2021, doi: 10.1088/1757-899x/1096/1/012049.

[23] K. Kacprzak, G. Liskiewicz, and K. Sobczak, "Numerical investigation of conventional and modified Savonius wind turbines," *Renew. Energy*, vol. 60, pp. 578–585, 2013, doi: 10.1016/j.renene.2013.06.009.

[24] M. Yusvika, A. Sutaji, A. R. Prabowo, F. Imaduddin, and S. Hadi, "Prediction of the Hydrodynamic Performance of an Elliptical Blade Savonius Turbine using Computational Fluid Dynamics," *IOP Conf. Ser. Mater. Sci. Eng.*, vol. 1096, no. 1, p. 012050, 2021, doi: 10.1088/1757-899x/1096/1/012050.

[25] A. Sanusi, S. Soeparman, S. Wahyudi, and L. Yuliati, "Experimental study of combined blade savonius wind turbine," *Int. J. Renew. Energy Res.*, vol. 6, no. 2, pp. 615–619, 2016, doi: 10.20508/ijrer.v6i2.3455.g6826.

[26] J. Thiyagaraj, I. Rahamathullah, G. Anbuchezhiyan, R. Barathiraja, and A. Ponshanmugakumar, "Influence of blade numbers, overlap ratio and modified blades on performance characteristics of the savonius hydro-kinetic turbine," *Mater. Today Proc.*, vol. 46, pp. 4047–4053, 2020, doi: 10.1016/j.matpr.2021.02.568.

[27] R. Tania, R. L. Florin, I. V. D. Adriana, M. Roxana, A. Ancuta, and D. Florin, "Experimental investigation on the influence of Overlap Ratio on Savonius Turbines Performance," *Int. J. Renew. Energy Res.*, vol. 8, no. 3, pp. 1791–1799, 2018, doi: 10.20508/ijrer.v8i3.7764.g7480.

[28] L. A. Gallo, E. L. Chica, and E. G. Flórez, "Numerical Optimization of the Blade Profile of a Savonius Type Rotor Using the Response Surface Methodology," *Sustain.*, vol. 14, no. 9, pp. 1–18, 2022, doi: 10.3390/su14095596.

[29] N. Alom and U. K. Saha, "Arriving at the optimum overlap ratio for an elliptical-bladed savonius rotor," *Proc. ASME Turbo Expo*, vol. 9, pp. 1–10, 2017, doi: 10.1115/GT2017-64137.

[30] P. K. Talukdar, A. Sardar, V. Kulkarni, and U. K. Saha, "Parametric analysis of model Savonius hydrokinetic turbines through experimental and computational investigations," *Energy Convers. Manag.*, vol. 158, no. January, pp. 36–49, 2018, doi: 10.1016/j.enconman.2017.12.011.

[31] F. A. Moreno Vásquez, T. F. De Oliveira, and A. C. P. Brasil Junior, "On the

electromechanical behavior of hydrokinetic turbines," *Energy Convers. Manag.*, vol. 115, pp. 60–70, 2016, doi: 10.1016/j.enconman.2016.02.039.

[32] M. Amiri, M. Kahrom, and A. R. Teymourtash, "Aerodynamic analysis of a three-bladed pivoted savonius wind turbine: Wind tunnel testing and numerical simulation," *J. Appl. Fluid Mech.*, vol. 12, no. 3, pp. 819–829, 2019, doi: 10.29252/JAFM.12.03.29324.

[33] A. D. Aliferis, M. S. Jessen, T. Bracchi, and R. J. Hearst, "Performance and wake of a Savonius vertical-axis wind turbine under different incoming conditions," *Wind Energy*, vol. 22, no. 9, pp. 1260–1273, 2019, doi: 10.1002/we.2358.

[34] R. E. Sheldahl, B. F. Blackwell, and L. V. Feltz, "Wind Tunnel Performance Data for Two- and Three-Bucket Savonius Rotors.," *J Energy*, vol. 2, no. 3, pp. 160–164, 1978, doi: 10.2514/3.47966.

[35] A. Damak, Z. Driss, and M. S. Abid, "Experimental investigation of helical Savonius rotor with a twist of 180°," *Renew. Energy*, vol. 52, pp. 136–142, 2013, doi: 10.1016/j.renene.2012.10.043.

[36] M. H. Nasef, W. A. El-Askary, A. A. AbdEL-hamid, and H. E. Gad, "Evaluation of Savonius rotor performance: Static and dynamic studies," *J. Wind Eng. Ind. Aerodyn.*, vol. 123, pp. 1–11, 2013, doi: 10.1016/j.jweia.2013.09.009.

[37] R. Eymard, E. Normale, and U. De Provence, "Finite Volume Methods Thierry Gallou ~ t," *Computing*, vol. VII, no. Part 3, 2000.

[38] R. Petrova, *Finite Volume Method – Powerful Means of Engineering Desing*, vol. M. 2012.

[39] R. Acharya, "Investigation of Differences in Ansys Solvers CFX and Fluent," *R. Inst. Technol.*, no. June, pp. 1–48, 2016.

[40] C. M. Rhie and W. L. Chow, "Numerical study of the turbulent flow past an airfoil with trailing edge separation," *AIAA J.*, vol. 21, no. 11, pp. 1525–1532, 1983, doi: 10.2514/3.8284.

[41] I. Ostos, I. Ruiz, M. Gajic, W. Gómez, A. Bonilla, and C. Collazos, "A modified novel blade configuration proposal for a more efficient VAWT using CFD tools," *Energy Convers. Manag.*, vol. 180, no. August 2018, pp. 733–746, 2019, doi: 10.1016/j.enconman.2018.11.025.

[42] W. Jeong and J. Seong, "Comparison of effects on technical variances of computational fluid dynamics (CFD) software based on finite element and finite volume methods," *Int. J. Mech.*

Sci., vol. 78, pp. 19–26, 2014, doi: 10.1016/j.ijmecsci.2013.10.017.

[43] N. Hasan, I. G. S. Tibba, F. T. Mosisa, and A. Daniel, "Ground tunnel as renewable energy utilization of ground energy as a source and sink for building heating and cooling," *AIP Conf. Proc.*, vol. 2018, no. September, 2018, doi: 10.1063/1.5058242.

[44] H. Khawaja and M. Moatamedi, "Semi-implicit method for pressure-linked equations (SIMPLE) ⇓ solution in MATLAB®," *Int. J. Multiphys.*, vol. 12, no. 4, pp. 313–325, 2018, doi: 10.21152/1750-9548.12.4.313.

[45] S. P. Venkatesan, S. Venkatesh, M. Sunil Kumar, S. Senthamizh Selvan, and Y. Sai, "Analysis of the blade profile of the Savonius wind turbine using computational fluid dynamics," *Int. J. Ambient Energy*, vol. 43, no. 1, pp. 142–148, 2022, doi: 10.1080/01430750.2019.1630305.

[46] SHARCNet, "Reporting mesh statistics," *ANSYS, Inc.*, pp. 1–16, 2008, [Online]. Available: https://romeo.univ-reims.fr/documents/fluent/tgrid/ug/chp15.pdf

[47] H. Jeong, S. Lee, and S. D. Kwon, "Blockage corrections for wind tunnel tests conducted on a Darrieus wind turbine," *J. Wind Eng. Ind. Aerodyn.*, vol. 179, no. June, pp. 229–239, 2018, doi: 10.1016/j.jweia.2018.06.002.

[48] I. Ross and A. Altman, "Wind tunnel blockage corrections: Review and application to Savonius vertical-axis wind turbines," *J. Wind Eng. Ind. Aerodyn.*, vol. 99, no. 5, pp. 523–538, 2011, doi: 10.1016/j.jweia.2011.02.002.

[49] V. Dossena, G. Persico, B. Paradiso, L. Battisti, S. Dell'Anna, A. Brighenti, and E. Benini, "An experimental study of the aerodynamics and performance of a vertical axis wind turbine in a confined and unconfined environment," Journal of Energy Resources Technology, vol. 137, no. 5, 2015.

[50] A. Rezaeiha, I. Kalkman, and B. Blocken, "CFD simulation of a vertical axis wind turbine operating at a moderate tip speed ratio: Guidelines for minimum domain size and azimuthal increment," *Renew. Energy*, vol. 107, pp. 373–385, 2017, doi: 10.1016/j.renene.2017.02.006.

[51] C. Study *et al.*, "COMPUTATIONAL STUDY OF SAVONIUS WIND TURBINE Submitted in partial fulfillment of requirements for the degree," 2013.

[52] Q. Mo, H. Guan, S. He, Y. Liu, and R. Guo, "Guidelines for the computational domain size

on an urban-scale VAWT," *J. Phys. Conf. Ser.*, vol. 1820, no. 1, 2021, doi: 10.1088/1742-6596/1820/1/012177.

[53] K. Sobczak, "Numerical investigations of an influence of the aspect ratio on the Savonius rotor performance," *J. Phys. Conf. Ser.*, vol. 1101, no. 1, 2018, doi: 10.1088/1742-6596/1101/1/012034.

[54] M. A. Kamoji, S. B. Kedare, and S. V. Prabhu, "Performance tests on helical Savonius rotors," *Renew. Energy*, vol. 34, no. 3, pp. 521–529, 2009, doi: 10.1016/j.renene.2008.06.002.

[55] A. Zakaria and M. S. N. Ibrahim, "Numerical performance evaluation of savonius rotors by flow-driven and sliding-mesh approaches," *Int. J. Adv. Trends Comput. Sci. Eng.*, vol. 8, no. 1, pp. 57–61, 2019, doi: 10.30534/ijatcse/2019/10812019.

[56] M. Zemamou, A. Toumi, K. Mrigua, and M. Aggour, "Modified design of savonius wind turbine blade for performance improvement," *Int. J. Innov. Technol. Explor. Eng.*, vol. 9, no. 1, pp. 1432–1437, 2019, doi: 10.35940/ijitee.A4202.119119.

[57] H. A. Hassan Saeed, A. M. Nagib Elmekawy, and S. Z. Kassab, "Numerical study of improving Savonius turbine power coefficient by various blade shapes," *Alexandria Eng. J.*, vol. 58, no. 2, pp. 429–441, 2019, doi: 10.1016/j.aej.2019.03.005.

[58] P. A. S. F. Da Silva, L. D. Shinomiya, T. F. De Oliveira, J. R. P. Vaz, A. L. A. Mesquita, and A. C. P. B. Junior, "Design of Hydrokinetic Turbine Blades Considering Cavitation," *Energy Procedia*, vol. 75, pp. 277–282, 2015, doi: 10.1016/j.egypro.2015.07.343.

[59] G. Saini and R. P. Saini, "A review on technology, configurations, and performance of cross-flow hydrokinetic turbines," *Int. J. Energy Res.*, vol. 43, no. 13, pp. 6639–6679, 2019, doi: 10.1002/er.4625.

[60] E. F. Moran, M. C. Lopez, N. Moore, N. Müller, and D. W. Hyndman, "Sustainable hydropower in the 21st century," *Proc. Natl. Acad. Sci. U. S. A.*, vol. 115, no. 47, pp. 11891–11898, 2018, doi: 10.1073/pnas.1809426115.

[61] T. S. A. Rengma and P. M. V. B. Subbarao, "Water Flow Velocity Driven Modified Savonius Hydrokinetic Turbine," *Int. J. Mech. Eng. Robot. Res.*, vol. 11, no. 5, pp. 296–303, 2022, doi: 10.18178/ijmerr.11.5.296-303.

[62] R. H. Van Els and A. C. P. B. Junior, "The Brazilian Experience with Hydrokinetic Turbines," *Energy Procedia*, vol. 75, pp. 259–264, 2015, doi: 10.1016/j.egypro.2015.07.328.

TEZ İZİN FORMU / THESIS PERMISSION FORM

PROGRAM / PROGRAM

Sürdürülebilir Çevre ve Enerji Sistemleri / Sustainable Environment and Energy Systems ☑

Siyaset Bilimi ve Uluslararası İlişkiler / Political Science and International Relations ☐

İngilizce Öğretmenliği / English Language Teaching ☐

Elektrik Elektronik Mühendisliği / Electrical and Electronics Engineering ☐

Bilgisayar Mühendisliği / Computer Engineering ☐

Makina Mühendisliği / Mechanical Engineering ☐

YAZARIN / AUTHOR

Soyadı / Surname : Ike-Offiah

Adı / Name : Chiedozie Augustine

Programı / Program : Sustainable Environment and Energy Systems

TEZİN ADI / TITLE OF THE THESIS (**İngilizce** / English) : Investigation and Modification of Savonius Hydrokinetic turbine for low water speeds.

TEZİN TÜRÜ / DEGREE**: Yüksek Lisans** / Master ✓ **Doktora** / PhD ☐

1. **Tezin tamamı dünya çapında erişime açılacaktır. /** Release the entire work immediately for access worldwide. ☐

2. Tez iki yıl süreyle erişime kapalı olacaktır. / Secure the entire work for patent and/or proprietary purposes for a period of **two years. *** ✓

3. Tez altı ay süreyle erişime kapalı olacaktır. / Secure the entire work for period of **six months**. ***** ☐

Yazarın imzası / Author Signature ..... **Tarih** / Date .....

Tez Danışmanı / Thesis Advisor Full Name: Assist. Prof. Dr. Ali Atashbar Orang

Tez Danışmanı İmzası / Thesis Advisor Signature: .....

Eş Danışmanı / Co-Advisor Full Name: Assoc. Prof. Dr. Elif Oğuz

Eş Danışmanı İmzası / Co-Advisor Signature: .....

Program Koordinatörü / Program Coordinator Full Name: Assoc. Prof. Dr. Ceren Ince

Program Koordinatörü İmzası / Program Coordinator Signature: .....